PREDICTION OF WAVE ATTENUATION BY VEGETATION AND SEAWEED

by

Nobuhisa Kobayashi, Andrew W. Raichle

and

Toshiyuki Asano

RESEARCH REPORT NO. CACR-91-07
August 1991

CENTER FOR APPLIED COASTAL RESEARCH

DEPARTMENT OF CIVIL ENGINEERING
UNIVERSITY OF DELAWARE
NEWARK, DELAWARE 19716

Table of Contents

ABSTRACT 1
ACKNOWLEDGEMENT 1
INTRODUCTION 2
FORMULATION OF PROBLEM 3
ANALYTICAL SOLUTION 6
TIME-AVERAGED ENERGY EQUATION 9
COMPARISON WITH EXPERIMENT 13
WAVE ATTENUATION BY SUBAERIAL VEGETATION 33
SUMMARY AND CONCLUSIONS 36
REFERENCES 37
APPENDIX A: COMPUTER PROGRAM FOR COMPUTING WAVE NUMBER AND EXPONENTIAL DECAY COEFFICIENT 39
APPENDIX B: REGRESSION ANALYSIS OF MEASURED WAVE HEIGHTS FOR EACH OF SIXTY TEST RUNS 44

List of Figures

FIG. 1. Definition Sketch. 4

FIG. 2. Artificial Seaweed Experiment by Asano et al. (1988). 15

FIG. 3. Measured Wave Heights Fitted to Exponential Decay Model. 19

FIG. 4. Normalized Wave Number k_r' and Ratio between Approximate and Exact Values of k_r' as a Function of ϵ for $d' = 0.5$ and $L_o' = 2$, 5, 8 and 13. 22

FIG. 5. Normalized Decay Coefficient k_i' and Ratio between Approximate and Exact Values of k_i' as a Function of ϵ for $d' = 0.5$ and $L_o' = 2$, 5, 8 and 13. 23

FIG. 6. Calibrated Values of Drag Coefficient C_D as a Function of Reynolds Number Re. 26

FIG. 7. Comparison between Measured and Computed Values of Normalized Wave Number k_r'. 31

FIG. 8. Comparison between Measured and Computed Values of Normalized Decay Coefficient k_i'. 32

FIG. 9. Normalized Wave Number k_r' and Ratio between Approximate and Exact Values of k_r' as a Function of ϵ with $L_o' = 2$, 10 and 90 for Subaerial Vegetation. 34

FIG. 10. Normalized Decay Coefficient k_i' and Ratio between Approximate and Exact Values of k_i' as a Function of ϵ with $L_o' = 2$, 10 and 90 for Subaerial Vegetation. 35

List of Tables

Table 1. Summary of Sixty Test Runs where N = Number of Strips per Unit Horizontal Area; h = Water Depth Above Strips; f = Wave Frequency; and C = Measured Phase Velocity. 16

Table 2. Wave Heights H_1, H_2, H_3 and H_4 Measured at x = 0, 2, 4 and 6 m, Respectively. 17

Table 3. Summary of Dimensionless Parameters for Sixty Test Runs where $\beta = bN\ H_o/2$; $d' = d/(d+h)$; $L'_o = g/[2\pi(d+h)f^2]$; $k'_r = k_r(d+h)$; $k'_i = k_i(d+h)$; and C_D = Calibrated Drag Coefficient. 21

Table 4. Approximate and Exact Values of k'_r and k'_i Together with Difference $e_r(\%)$ Defined as e_r = 100 (Approximate Value–Exact Value)/(Exact Value) for Calibrated C_D. 25

Table 5. Calibrated and Empirical Values of Drag Coefficient C_D Together with Characteristic Fluid Velocity u_c and Reynolds Number Re for Each of Sixty Test Runs. 28

Table 6. Computed Exact Values of k'_r and k'_i Using Empirical Value of C_D as Compared with Measured Values of k'_r and k'_i for Each Run. 29

Table 7. Approximate and Exact Values of k'_r and k'_i Together with Difference $e_r(\%)$ Defined as e_r = 100 (Approximate Value–Exact Value)/(Exact Value) for Empirical C_D. 30

ABSTRACT

The vertically two-dimensional problem of small-amplitude waves propagating over submerged vegetation is formulated using the continuity and linearized momentum equations for the regions with and without the vegetation. The effects of the vegetation on the flow field are assumed to be expressible in terms of the drag force acting on the vegetation. An analytical solution is obtained for the monochromatic wave whose height decays exponentially. The expressions for the wave number and the exponential decay coefficient derived for arbitrary damping are shown to reduce to those based on linear wave theory and the conservation equation of energy if the damping is small. The analytical solution is compared with sixty test runs conducted using deeply submerged artificial seaweed. The calibrated drag coefficients for these runs are found to vary in a wide range and appear to be affected by the seaweed motion and viscous effects neglected in the analysis. The analytical solution is also shown to be applicable to subaerial vegetation, which is predicted to be much more effective in dissipating wave energy.

ACKNOWLEDGEMENT

This study was partly supported by the Monbusho International Scientific Research Program (Joint Research), No. 02044149, of the Japanese Ministry of Education, Science and Culture.

INTRODUCTION

Wave attenuation by vegetation has been investigated in relation to prediction of wind waves propagating across flooded, vegetated lands (e.g., Camfield 1977; Shore Protection Manual 1984) as well as possible use of artificial seaweed in promoting the build-up of beaches (e.g., Price et al. 1968; Asano et al. 1988). Dalrymple et al. (1984) examined wave diffraction due to localized areas of energy dissipation, which might be dense stands of seaweed, pile clusters, or submerged trees. The detailed mechanisms of wave attenuation by vegetation is not well understood partly because of difficulties in analyzing the flow field in the vegetation field and partly because of lack of comprehensive data. The need of improved understanding of the mechanisms may increase since accelerated sea level rise may result in more flooding in vegetated areas (ASCE Task Committee on sea level rise and its effects on bays and estuaries 1992).

A standard approach for predicting wave attenuation by vegetation is based on the time-averaged conservation equation of wave energy in which the local flow field is estimated using linear wave theory. The effects of the vegetation are included only in the dissipation term in the energy equation used to obtain the local wave height. This simple approach is intuitive and may not be justified if the vegetation modifies the local flow field significantly. This paper presents a different approach based on the continuity and momentum equations. First, the problem of small-amplitude waves propagating over submerged vegetation without lateral boundaries is formulated assuming that the problem is two-dimensional vertically. Second, an analytical solution is obtained for the small-amplitude monochromatic wave whose height decays exponentially in the direction of wave propagation. Third, the time-averaged energy equation derived from the adopted momentum equations is shown to reduce to the standard energy equation based on linear wave theory if the damping is small. Fourth, the analytical solution is compared with the artificial seaweed experiment conducted by Asano et al. (1988). Finally, the analytical solution obtained for submerged vegetation is shown to be applicable to subaerial vegetation as well.

FORMULATION OF PROBLEM

The two-dimensional problem examined herein is depicted in Fig. 1 where x = horizontal coordinate taken to be positive in the direction of wave propagation; z = vertical coordinate taken to be positive upward with $z = 0$ at the still water level (SWL); d = constant height of submerged vegetation in the absence of waves; h = still water depth above the vegetation; η_1 = free surface elevation above SWL; η_2 = vertical displacement of the interface between the two regions with and without the vegetation. The bottom located at $z = -(d + h)$ is assumed to be horizontal. In Fig. 1, u = horizontal fluid velocity; w = vertical fluid velocity; and p = dynamic pressure where the subscripts 1 and 2 indicate the regions above and below the interface located at $z = (\eta_2 - h)$. The total pressure is the sum of the dynamic pressure and the hydrostatic pressure $(-\rho g z)$ below SWL where ρ = fluid density which is assumed constant; and g = gravitational acceleration. In the following, small-amplitude monochromatic waves are assumed to propagate in the positive x-direction and be attenuated by the vegetation.

In the region $(\eta_2 - h) < z < \eta_1$ without the vegetation, the continuity equation is given by

$$\frac{\partial u_1}{\partial x} + \frac{\partial w_1}{\partial z} = 0 \tag{1}$$

As a first approximation, the fluid convective accelerations and stresses are assumed to be negligible in this region. The linearized horizontal and vertical momentum equations may be expressed as

$$\rho \frac{\partial u_1}{\partial t} = -\frac{\partial p_1}{\partial x} \tag{2}$$

$$\rho \frac{\partial w_1}{\partial t} = -\frac{\partial p_1}{\partial z} \tag{3}$$

in which t = time. Eqs. 2 and 3 correspond to the linearized Euler equations (e.g., Dean and Dalrymple 1984). The linearized kinematic and dynamic boundary conditions at the free surface are written as

$$\frac{\partial \eta_1}{\partial t} = w_1 \qquad \text{at } z = 0 \tag{4}$$

$$p_1 = \rho g \eta_1 \qquad \text{at } z = 0 \tag{5}$$

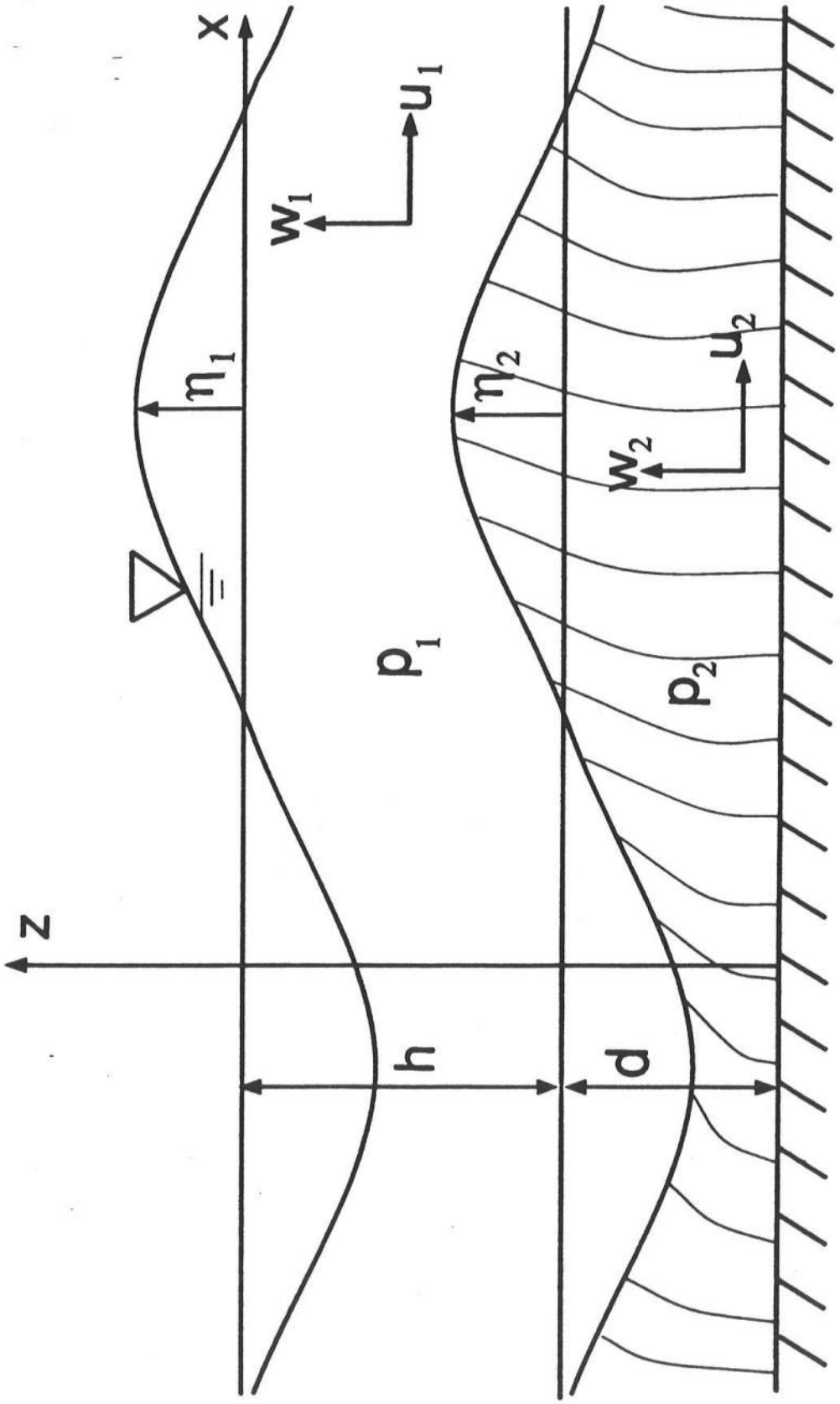

FIG. 1. Definition Sketch.

where the effects of wind are not considered herein.

In the region $-(h+d) < z < (\eta_2 - h)$ with the vegetation, the continuity equation is given by

$$\frac{\partial u_2}{\partial x} + \frac{\partial w_2}{\partial z} = 0 \tag{6}$$

The horizontal and vertical momentum equations including the effects of the vegetation may be expressed as

$$\rho \frac{\partial u_2}{\partial t} = -\frac{\partial p_2}{\partial x} - F_x \tag{7}$$

$$\rho \frac{\partial w_2}{\partial t} = -\frac{\partial p_2}{\partial z} - F_z \tag{8}$$

in which F_x and F_z are the horizontal and vertical forces acting on the vegetation per unit volume. The kinematic boundary condition on the horizontal bottom is given by

$$w_2 = 0 \qquad \text{at} \quad z = -(h+d) \tag{9}$$

where the bottom is assumed to be impermeable.

To estimate the forces F_x and F_z, the vegetation may simply be regarded as rigid vertical cylinders with small diameters for which the drag force is dominant (Dalrymple et al. 1984). Accordingly, F_x and F_z may be approximated by

$$F_x \simeq \frac{1}{2}\rho\, C_D\, b\, N\, |u_2|\, u_2 \tag{10}$$

$$F_z \simeq 0 \tag{11}$$

in which C_D = drag coefficient; b = area per unit height of each vegetation stand normal to u_2; and N = number of vegetation stands per unit horizontal area. In reality, the horizontal velocity, u_2, in Eq. 10 should be the horizontal fluid velocity relative to the horizontal velocity of the vegetation stand, but the motion of the vegetation is not analyzed herein. Consequently, the drag coefficient C_D in Eq. 10 includes the effect of the vegetation motion as will be discussed when C_D is calibrated using the experiment of Asano et al. (1988).

On the other hand, the linearized kinematic boundary condition at the interface between the two regions is written as

$$\frac{\partial \eta_2}{\partial t} = w_1 \qquad \text{at } z = -h \tag{12}$$

The linearized matching conditions at the interface are expressed as

$$w_1 = w_2 \qquad \text{at } z = -h \tag{13}$$

$$p_1 = p_2 \qquad \text{at } z = -h \tag{14}$$

The horizontal velocities u_1 and u_2 do not match at the interface since the horizontal momentum equation changes abruptly from Eq. 2 to Eq. 7 where F_x given by Eq. 10 is non-zero. To match u_1 and u_2 at the interface, the shear stress would need to be accounted for in Eqs. 2 and 7.

ANALYTICAL SOLUTION

Eqs. 1, 2, 3, 6, 7 and 8 with Eqs. 10 and 11 and the conditions given by Eqs. 4, 5, 9, 12, 13 and 14 may be solved to obtain η_1, u_1, w_1, p_1, η_2, u_2, w_2 and p_2. In order to derive an analytical solution, Eq. 10 is linearized as follows:

$$F_x \simeq \rho\, D\, u_2 \tag{15}$$

where the unknown coefficient D will later be determined using the time-averaged equation of wave energy. Furthermore, the free surface displacement η_1 is assumed to be expressible in the form

$$\eta_1 = \frac{H_o}{2} \exp(-k_i x) \cos(k_r x - \omega t) \tag{16}$$

in which H_o = wave height at $x = 0$; k_i = exponential decay coefficient; k_r = wave number; and ω = angular frequency. In this problem, k_i and k_r are unknown, whereas H_o and ω are given. Eq. 16 assumes that the small-amplitude monochromatic wave propagates in the positive x-direction with the phase velocity, $c = \omega/k_r$, and the local wave height, H, decays exponentially

$$H = H_o \exp(-k_i x) \tag{17}$$

To solve the linearized problem, it is convenient to introduce the complex wave number, k, defined as

$$k = k_r + i k_i \tag{18}$$

in which $i = \sqrt{-1}$. Moreover, Eq. 16 is rewritten as

$$\eta_1 = R_e \left\{ \frac{H_o}{2} \exp\left[i(kx - \omega t)\right] \right\} \tag{19}$$

where R_e indicates the real part of the complex function in the brackets and will be omitted hereafter. In this simplified analysis, u_1, w_1, p_1, η_2, u_2, w_2 and p_2 are also proportional to $\exp[i(kx - \omega t)]$ which specifies the horizontal and temporal variations.

For the region without the vegetation, Eqs. 2 and 3 are used to express u_1 and w_1 in terms of p_1

$$u_1 = \frac{k}{\rho\omega} p_1 \tag{20}$$

$$w_1 = -\frac{i}{\rho\omega} \frac{\partial p_1}{\partial z} \tag{21}$$

Substituting Eqs. 20 and 21 into Eq. 1 and solving the resulting equation with the free surface boundary conditions given by Eqs. 4 and 5, p_1 is given by

$$p_1 = \rho g \frac{H_o}{2} \left[\cosh(kz) + \frac{\omega^2}{kg} \sinh(kz) \right] \exp\left[i(kx - \omega t)\right] \tag{22}$$

Substitution of Eq. 22 into Eqs. 20 and 21 yields the explicit expressions of u_1 and w_1 which are omitted herein. Furthermore, Eq. 12 yields the vertical displacement of the interface

$$\eta_2 = \frac{H_o}{2} \left[\cosh(kh) - \frac{kg}{\omega^2} \sinh(kh) \right] \exp\left[i(kx - \omega t)\right] \tag{23}$$

If $\omega^2 = kg \tanh(kh)$, $\eta_2 = 0$, $k = k_r$ with $k_i = 0$, and Eqs. 20, 21 and 22 reduce to the standard expressions for constant water depth h based on linear wave theory with no damping (e.g., Dean and Dalrymple 1984).

For the region with the vegetation, Eqs. 7 and 8 with Eqs. 11 and 15 yield

$$u_2 = \frac{k}{\rho(\omega + iD)} p_2 \tag{24}$$

$$w_2 = -\frac{i}{\rho\omega} \frac{\partial p_2}{\partial z} \tag{25}$$

Substituting Eqs. 24 and 25 into Eq. 6 and solving the resulting equation with the conditions given by Eqs. 9 and 13, p_2 is given by

$$p_2 = \rho g \frac{H_o}{2} \left[\cosh(kh) - \frac{\omega^2}{kg} \sinh(kh) \right] \frac{\cosh[\alpha(z + h + d)]}{\cosh(\alpha d)} \exp\left[i(kx - \omega t)\right] \tag{26}$$

with

$$\alpha^2 = \frac{\omega k^2}{\omega + iD} \tag{27}$$

Lastly, the matching condition given by Eq. 14 yields the equation for the unknown complex wave number k defined by Eq. 18

$$\omega^2 = kg\frac{k\tanh(kh) + \alpha\tanh(\alpha d)}{k + \alpha\tanh(\alpha d)\tanh(kh)} \tag{28}$$

which may be solved to find k for given ω, h, d, D and g.

The coefficient D introduced in Eq. 15 indicates the degree of damping of wave energy caused by the drag force F_x acting on the vegetation. For the case of $D = 0$, the solution derived herein can be shown to reduce to the solution for constant water depth $(h+d)$ based on linear wave theory with no damping. To simplify Eq. 28 for the case of weak damping, it is convenient to introduce the dimensionless damping coefficient ϵ defined as

$$\epsilon = \frac{D}{2\omega} \tag{29}$$

For the case of $\epsilon \ll 1$, the terms of the order of ϵ^2 and smaller may be neglected and Eq. 27 is approximated by

$$\alpha \simeq k(1 - i\epsilon) \tag{30}$$

Substituting Eq. 30 with Eq. 18 into Eq. 28 and performing lengthy algebraic manipulations, the real wave number k_r and the exponential decay coefficient $k_i = \delta k_r$ for the case of $\epsilon \ll 1$ are approximately expressed as

$$\omega^2 \simeq k_r g \tanh\left[k_r(h + d)\right] \tag{31}$$

$$\delta = \frac{k_i}{k_r} \simeq \epsilon\,\frac{2k_r d + \sinh(2k_r d)}{2k_r(h + d) + \sinh[2k_r(h + d)]} \tag{32}$$

Eq. 31 is the dispersion relationship based on linear wave theory and weak damping with $\epsilon \ll 1$ does not affect the real wave number k_r and the phase velocity $c = \omega/k_r$. Eq. 32 shows that $\delta = (k_i/k_r)$ is proportional to $\epsilon \ll 1$. For the case of weak damping, the horizontal length scale, k_i^{-1}, associated with wave attenuation is hence large relative to the wavelength $2\pi/k_r$. It will be shown in the next section that Eq. 32 can also be derived from the standard conservation equation of wave energy.

For the computation of k_r and k_i using Eqs. 28, 31 and 32, the dimensional parameters are normalized by the water depth $(d+h)$ as follows:

$$k'_r = k_r(d+h) \;\; ; \;\; k'_i = k_i(d+h) \;\; ; \;\; L'_o = \frac{2\pi g}{\omega^2(d+h)} \;\; ; \;\; d' = \frac{d}{d+h} \tag{33}$$

where the prime indicates the dimensionless parameters and L'_o is the normalized wavelength in deep water. The approximate value of k'_r for $\epsilon \ll 1$ is computed for given L'_o using Eq. 31. The approximate value of k'_i for $\epsilon \ll 1$ is calculated for given L'_o, d' and ϵ using Eq. 32. The values of k'_r and k'_i for arbitrary ϵ are computed for given L'_o, d' and ϵ using Eq. 28 with Eq. 27 where use is made of a Newton-Raphson iteration method (e.g., Press et al. 1986) starting from the approximate values of k'_r and k'_i for $\epsilon \ll 1$. The iteration method has been found to converge for the computed results presented later in this report, although the convergence has not been proven mathematically. The computer program is attached in Appendix A.

TIME-AVERAGED ENERGY EQUATION

The time-averaged equation of wave energy is derived herein to obtain the expression of the damping coefficient D introduced in Eq. 15. It will also be shown that the approximate expression of k_i for $\epsilon \ll 1$ given by Eq. 32 can also be derived from the standard conservation equation of wave energy based on the flow field estimated using linear wave theory (Dalrymple et al. 1984).

To derive the time-averaged energy equation for the region with no vegetation, Eqs. 2 and 3 are multiplied by u_1 and w_1, respectively. The multiplied equations are added and integrated from $z = -h$ to $z = 0$. The integrated equation is time-averaged and simplified using Eqs. 4 and 5. The resulting time-averaged energy equation is expressed as

$$\frac{dF_1}{dx} = -P \tag{34}$$

with

$$F_1 \;\; = \;\; \int_{-h}^{0} \overline{u_1 p_1} \, dz \tag{35}$$

$$P = -\overline{w_1 p_1} \quad \text{at } z = -h \tag{36}$$

where the overbar indicates the time averaging. F_1 is the time-averaged energy flux per unit width in the region without the vegetation, while P is the time-averaged rate of work by the dynamic pressure p_1 on the unit area of the interface between the two regions. It is noted that u_1, w_1 and p_1 given by Eqs. 20, 21 and 22 should satisfy Eq. 34 with Eqs. 35 and 36 derived from Eqs. 2 and 3.

Likewise, Eqs. 7 and 8 with $F_z = 0$ from Eq. 11 are multiplied by u_2 and w_2, respectively. The multiplied equations are added and integrated from $z = -(h+d)$ to $z = -h$ using Eqs. 9, 13 and 14. The integrated equation is time-averaged to obtain the following energy equation for the region with the vegetation.

$$\frac{dF_2}{dx} = P - D_d \tag{37}$$

with

$$F_2 = \int_{-(h+d)}^{-h} \overline{u_2 p_2}\, dz \tag{38}$$

$$D_d = \int_{-(h+d)}^{-h} \overline{u_2 F_x}\, dz \tag{39}$$

where F_2 = time-averaged energy flux per unit width in the vegetated region; and D_d = time-averaged rate of energy dissipation per unit horizontal area due to the drag force F_x. It is noted that u_2, w_2 and p_2 given by Eqs. 24, 25 and 26 should satisfy Eq. 37 with Eqs. 38 and 39 derived from Eqs. 7 and 8 with Eqs. 11 and 15.

The time-averaged energy equation for the entire water depth $(d + h)$ is obtained by adding Eqs. 34 and 37

$$\frac{d}{dx}(F_1 + F_2) = -D_d \tag{40}$$

in which $(F_1 + F_2)$ is the time-averaged energy flux per unit width in both regions. The dissipation rate D_d defined by Eq. 39 depends on the equation used to express F_x. Substitution of the nonlinear expression of F_x given by Eq. 10 into Eq. 39 yields

$$D_d \simeq \frac{1}{2}\rho\, C_D\, b\, N \int_{-(h+d)}^{-h} \overline{|u_2| u_2^2}\, dz \tag{41}$$

On the other hand, substitution of the linear expression of F_x given by Eq. 15 into Eq. 39 yields

$$D_d \simeq \rho D \int_{-(h+d)}^{-h} \overline{u_2^2}\, dz \tag{42}$$

The horizontal velocity u_2 in Eqs. 41 and 42 is the real part of Eq. 24 with p_2 being given by Eq. 26. The unknown damping coefficient D introduced in Eq. 15 to obtain the analytical solution may be chosen such that D_d given by Eq. 41 becomes approximately the same as D_d given by Eq. 42. The explicit expression of D for the case of weak damping will later be obtained in this way.

For the case of weak damping where the dimensionless damping coefficient ϵ defined by Eq. 29 is much less than unity, Eq. 28 for $k = (k_r + ik_i)$ has been shown to be simplified as Eqs. 31 and 32 where $\delta = (k_i/k_r)$ is of the order ϵ. In the following, the expressions for F_1, P, F_2 and D_d for the case of $\epsilon \ll 1$ are obtained to elucidate the effects of the vegetation on the flow field and the time-averaged energy quantities.

For the case of $\epsilon \ll 1$, Eq. 22 with $k = k_r(1 + i\delta)$ can be shown to be approximated as

$$p_1 \simeq \rho g \frac{H}{2} \left\{ \frac{\cosh\left[k_r(h+d+z)\right]}{\cosh\left[k_r(h+d)\right]} + i\delta c_1 \right\} \exp\left[i(k_r x - \omega t)\right] \tag{43}$$

with

$$c_1 = \frac{k_r z \sinh\left[k_r(h+d+z)\right]}{\cosh\left[k_r(h+d)\right]} - \sinh(k_r z)\tanh\left[k_r(h+d)\right] \tag{44}$$

where the local wave height H is defined by Eq. 17. If $c_1 = 0$, Eq. 43 would express the dynamic pressure in the water depth $(h + d)$ based on linear wave theory (e.g., Dean and Dalrymple 1984). Substitution of Eq. 43 into Eqs. 20 and 21 yields the approximate expressions of u_1 and w_1 to the order ϵ. Substitution of the real parts of these approximate expressions into Eqs. 35 and 36 yields

$$F_1 \simeq cE \left\{ \frac{c_g}{c} - \frac{2k_r d + \sinh(2k_r d)}{2\sinh[k_r(h+d)]} \right\} \tag{45}$$

$$P \simeq 2\, k_i\, F_1 \tag{46}$$

with

$$E = \frac{1}{8}\rho\, g\, H^2 \tag{47}$$

$$c_g = \frac{c}{2}\left[1 + \frac{2k_r(h+d)}{\sinh[2k_r(h+d)]}\right] \tag{48}$$

where E and c_g are the local wave energy per unit horizontal area and the wave group velocity in the water depth $(h+d)$ based on linear wave theory. Eqs. 45 and 46 can be shown to satisfy Eq. 34. F_1 given by Eq. 45 turns out to be the same as F_1 obtained using the expressions of p_1 and u_1 based on linear wave theory.

Likewise, for the case of $\epsilon \ll 1$, Eq. 26 with $k = k_r(1+i\delta)$ and $\alpha \simeq k_r[1+i(\delta-\epsilon)]$ from Eq. 30 can be shown to be approximated as

$$p_2 \simeq \rho g \frac{H}{2} \frac{\cosh[k_r(h+d+z)]}{\cosh[k_r(h+d)]} [1 + i\delta c_2 + i(\delta-\epsilon)c_3] \exp[i(k_r x - \omega t)] \tag{49}$$

with

$$c_2 = \frac{\sinh(k_r h)\sinh[k_r(h+d)]}{\cosh(k_r d)} - k_r h \tanh(k_r d) \tag{50}$$

$$c_3 = k_r(h+d+z)\tanh[k_r(h+d+z)] - k_r d \tanh(k_r d) \tag{51}$$

If $c_2 = 0$ and $c_3 = 0$, Eq. 49 would express the dynamic pressure based on linear wave theory. Substitution of Eq. 49 into Eqs. 24 and 25, where $k/(\omega + iD) \simeq k_r[1+i(\delta-2\epsilon)]/\omega$ to the order $\epsilon = D/(2\omega)$, yields the approximate expressions of u_2 and w_2 to the order ϵ. Substitution of the real parts of these approximate expressions into Eqs. 38, 41 and 42 yields

$$F_2 \simeq cE\frac{2k_r d + \sinh(2k_r d)}{2\sinh[2k_r(h+d)]} \tag{52}$$

$$D_d \simeq \frac{2}{3\pi}\rho C_D b N \left(\frac{k_r g H}{2\omega}\right)^3 \frac{\sinh^3(k_r d) + 3\sinh(k_r d)}{3k_r \cosh^3[k_r(h+d)]} \tag{53}$$

$$D_d \simeq D E \frac{2k_r d + \sinh(2k_r d)}{2\sinh[2k_r(h+d)]} \tag{54}$$

where Eqs. 53 and 54 correspond to the nonlinear and linear expressions of F_x given by Eqs. 10 and 15, respectively. Eqs. 52, 53 and 54 turn out to be the same as those obtained using the expressions of p_2 and u_2 based on linear wave theory.

Substituting Eqs. 45 and 52 into Eq. 40, the time-averaged energy equation for the entire water depth for the case of weak damping is approximated as

$$\frac{d}{dx}\left(E\, c_g\right) \simeq -D_d \tag{55}$$

which is the standard conservation equation of wave energy based on linear wave theory (Dalrymple et al. 1984). Substitution of Eqs. 47, 48 and 54 based on linear wave theory into Eq. 55 yields the exponential decay of the local wave height H given by Eq. 17 with k_i being expressed by Eq. 32 for the case of $\epsilon \ll 1$ which has been obtained using the linear expression of F_x given by Eq. 15. Consequently, use of Eq. 55 to find the decay of the local wave height H is justified for the case of weak damping. However, Eqs. 43 and 49 show that the flow field is affected by the presence of the vegetation even for the case of weak damping.

Finally, an approximate expression of the unknown constant D is obtained using Eqs. 53 and 54. D_d is proportional to H^3 and H^2 in Eqs. 53 and 54, respectively, where E is defined by Eq. 47. Consequently, the horizontal variations of D_d given by Eqs. 53 and 54 can not be matched exactly. Since Eqs. 53 and 54 are applicable for the case of $\epsilon = D/(2\omega) \ll 1$, H^3 in Eq. 53 may be approximated as $H^2 H_o$ where $H = H_o$ at $x = 0$ from Eq. 17. Equating Eqs. 53 and 54 under this approximation, the following approximate expression of ϵ is obtained

$$\epsilon = \frac{D}{2\omega} \simeq \frac{1}{9\pi} C_D\, b\, N\, H_o\, \frac{\sinh(3k_r d) + 9\sinh(k_r d)}{[2k_r d + \sinh(2k_r d)]\sinh[k_r(h+d)]} \tag{56}$$

where k_r is given by Eq. 31 for $\epsilon \ll 1$. Strictly speaking, Eq. 56 is valid only for $\epsilon \ll 1$ but may tentatively be used as long as ϵ is not too large. This is because ϵ in Eq. 56 is proportional to the drag coefficient C_D which is a very uncertain parameter as will be shown in the next section.

COMPARISON WITH EXPERIMENT

The analytical solution obtained herein is compared with the artificial seaweed experiment conducted by Asano et al. (1988). The experiment was performed in a wave tank which was 27 m long, 0.5 m wide and 0.7 m high. The artificial seaweed was made of polypropylene

strips whose specific gravity was 0.9. The length, width and thickness of each strip was d = 25 cm, b = 5.2 cm and 0.03 mm, respectively. Each strip was bound to a heavy wire netting such that the strip was normal to the side walls of the tank and could bend with little torsion under the action of monochromatic waves generated in the tank. The strips were placed across the bottom over the distance of 8 m in the middle section of the tank as shown in Fig. 2. The number of strips placed uniformly over the area of 4 m^2 was 4400 and 5960. Correspondingly, the number of strips per unit horizontal area was N = 0.110 and 0.149 cm^{-2}. The water depth above the vertical strips was h = 20 and 27 cm. The total water depth in the tank was $(h + d)$ = 45 and 52 cm. Out of the four possible combinations of N and h, the case of N = 0.149 cm^{-2} and h = 27 cm was not tested in this experiment.

For each of the three combinations of N and h, the wave frequency, $f = \omega/(2\pi)$, of the monochromatic waves generated in the tank was selected as f = 0.5, 0.6, 0.7, 0.8, 0.9, 1.0, 1.2 and 1.4 Hz. The typical number of different wave heights generated in the tank was six for f = 0.8 Hz and two for the rest of the wave frequencies. In total, sixty test runs were performed as summarized in Table 1.

For each of the sixty test runs, capacitance wave gages were used to measure the free surface oscillations at four locations above the artificial seaweed as shown in Fig. 2. The distance between the two adjacent gages was 2 m. The first gage was located 1 m from the seaward edge of the seaweed field. This location of the first gage is taken herein to be the location x = 0 for the analytical solution since the present analysis does not account for the presence of the lateral boundaries. The four gages are hence located at x = 0, 2, 4 and 6 m in the following data analysis. The data for each run includes the wave height H measured at these four locations as shown in Table 2 and the phase velocity c which was calculated using the measured travel time of the wave crests between the wave gages. The measured phase velocities were not very accurate partly because of difficulty in pinpointing the arrival time of the wave crests. Discarding unreliable measurements, the measured value of the phase velocity c was available for 52 runs as listed in Table 1. The measured values of c were in the range 1.08–1.69 m/s. The corresponding values of $k_r = (2\pi f)/c$ were in the range 2.07–8.14 m^{-1}.

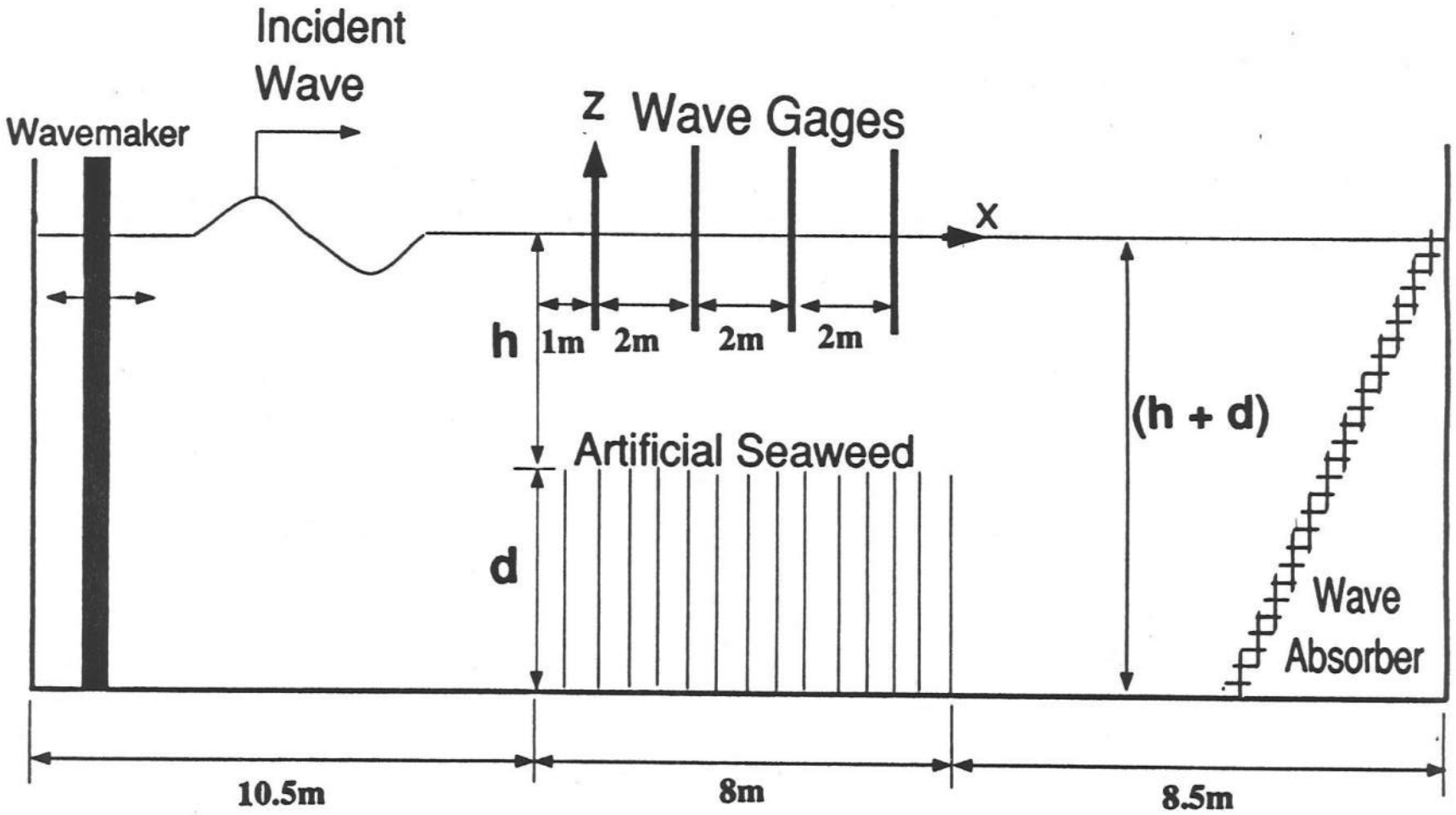

FIG. 2. Artificial Seaweed Experiment by Asano et al. (1988).

Table 1: Summary of Sixty Test Runs where N = Number of Strips per Unit Horizontal Area; h = Water Depth Above Strips; f = Wave Frequency; and C = Measured Phase Velocity.

Run #	N (cm^{-2})	h (cm)	f (Hz)	C (cm/s)
1	0.149	20	0.500	no value
2	0.149	20	0.600	155
3	0.149	20	0.600	148
4	0.149	20	0.700	163
5	0.149	20	0.700	167
6	0.149	20	0.800	167
7	0.149	20	0.800	no value
8	0.149	20	0.800	167
9	0.149	20	0.800	155
10	0,149	20	0.800	no value
11	0.149	20	0.800	no value
12	0.149	20	0.800	no value
13	0.149	20	0.800	no value
14	0.149	20	0.800	no value
15	0.149	20	0.800	no value
16	0.149	20	0.900	154
17	0.149	20	0.900	151
18	0.149	20	1.000	138
19	0.149	20	1.000	139
20	0.149	20	1.200	131
21	0.149	20	1.200	132
22	0.149	20	1.400	114
23	0.149	27	0.500	144
24	0.149	27	0.500	152
25	0.149	27	0.600	161
26	0.149	27	0.600	162
27	0.149	27	0.700	165
28	0.149	27	0.700	166
29	0.149	27	0.800	169
30	0.149	27	0.800	167
31	0.149	27	0.800	165
32	0.149	27	0.800	164
33	0.149	27	0.800	167
34	0.149	27	0.800	166
35	0.149	27	0.900	158
36	0.149	27	0.900	157
37	0.149	27	1.000	151
38	0.149	27	1.000	147
39	0.149	27	1.200	127
40	0.149	27	1.200	124
41	0.149	27	1.400	108
42	0.110	20	0.500	145
43	0.110	20	0.500	147
44	0.110	20	0.600	154
45	0.110	20	0.600	154
46	0.110	20	0.700	162
47	0.110	20	0.700	162
48	0.110	20	0.800	164
49	0.110	20	0.800	160
50	0.110	20	0.800	162
51	0.110	20	0.800	162
52	0.110	20	0.800	160
53	0.110	20	0.800	158
54	0.110	20	0.900	152
55	0.110	20	0.900	148
56	0.110	20	1.000	145
57	0.110	20	1.000	143
58	0.110	20	1.200	124
59	0.110	20	1.200	124
60	0.110	20	1.400	111

Table 2: Wave Heights H_1, H_2, H_3 and H_4 Measured at $x = 0, 2, 4$ and 6 m, Respectively.

Run #	H_1 (cm)	H_2 (cm)	H_3 (cm)	H_4 (cm)
1	3.8	3.1	2.9	2.9
2	10.8	9.5	7.4	6.5
3	7.2	6.4	5.0	4.4
4	13.6	10.7	9.7	7.7
5	8.4	7.1	6.6	5.2
6	14.7	11.6	9.9	8.5
7	8.9	7.2	6.7	5.7
8	19.3	15.3	12.8	11.1
9	18.4	13.7	11.3	10.0
10	14.0	11.4	9.8	8.5
11	12.2	10.0	8.5	8.2
12	10.6	8.9	7.5	6.7
13	8.9	7.2	6.2	5.6
14	7.4	6.0	5.4	4.7
15	5.0	4.1	3.9	3.5
16	14.0	11.5	10.0	9.0
17	8.2	7.2	6.4	5.8
18	13.8	12.7	11.7	10.4
19	9.0	8.0	7.5	7.1
20	9.8	8.4	8.5	8.0
21	6.6	6.0	5.5	5.3
22	8.2	7.0	6.9	6.5
23	8.6	8.1	7.0	6.3
24	5.5	5.2	4.7	4.3
25	11.5	9.8	8.5	8.8
26	6.9	6.4	5.2	5.7
27	14.4	13.2	11.3	10.7
28	9.3	8.3	7.4	7.0
29	19.0	17.6	15.4	13.3
30	16.6	15.4	13.6	12.1
31	13.9	13.3	12.1	10.6
32	11.9	11.8	10.3	9.2
33	9.6	9.1	8.3	7.6
34	6.8	6.8	6.0	5.6
35	17.1	15.7	14.6	13.1
36	11.7	10.5	9.6	9.0
37	16.9	16.1	14.9	13.8
38	9.2	9.4	8.9	7.7
39	11.9	11.9	10.7	10.0
40	7.4	7.6	7.0	6.8
41	7.8	8.1	7.6	7.0
42	6.5	5.5	5.5	5.1
43	4.1	3.5	3.4	3.5
44	10.0	8.8	7.1	6.5
45	6.0	5.5	4.7	4.4
46	12.3	10.2	9.7	8.4
47	7.3	6.0	6.3	5.5
48	16.5	14.0	13.1	11.8
49	14.5	12.5	11.4	10.6
50	12.8	11.1	10.5	9.8
51	11.3	9.8	9.0	8.1
52	9.0	7.8	7.3	6.9
53	7.0	6.3	5.9	5.6
54	14.5	13.1	12.2	11.0
55	9.2	8.3	7.6	7.2
56	15.3	14.0	13.5	13.0
57	8.7	8.3	8.0	7.6
58	11.7	10.5	10.1	10.0
59	6.1	5.8	5.9	5.5
60	6.9	6.4	6.3	6.0

A regression analysis based on the method of least squares (e.g., Press et al. 1986) is performed using Eq. 17 in which the exponential decay of the local wave height H is characterized by the wave height H_o at $x = 0$ and the exponential decay coefficient k_i. For each run, the fitted values of H_o and k_i are obtained from the measured wave heights at x = 0, 2, 4 and 6 m as shown in Appendix B. The fitted values of H_o and k_i for the sixty runs are in the ranges H_o = 3.6–19.4 cm and k_i = 0.015– 0.101 m^{-1}. The correlation coefficients for the sixty runs vary from 0.780 to 0.998 and the average value is 0.959.

Fig. 3 shows the measured values of H at x = 0, 2, 4 and 6 m for the sixty runs normalized as H/H_o as a function of $k_i x$ where the fitted values of H_o and k_i are used for each run. The data points in Fig. 3 fall within ± 10% of the theoretical line based on $H/H_o = \exp(-k_i x)$. This suggests that the wave attenuation in the region $0 \leq x \leq 6$ m may not have been affected much by the lateral boundaries located at $x = -1$ and 7 m as shown in Fig. 2. It should also be stated that the measured wave attenuation included the effect of the bottom and side-wall friction neglected in the present analysis. Wave attenuation in the absence of the artificial seaweed was not measured in this experiment, but the values of k_i due to the bottom and side-wall friction for these test runs were estimated to be of the order 0.003 m^{-1} using the laminar boundary layer model of Iwagaki and Tsuchiya (1966). These estimates did not account for the wire netting placed at the bottom. At the location x = 6 m, $\exp(-k_i x) = 0.98$ for k_i = 0.003 m^{-1} as compared to $\exp(-k_i x)$ = 0.55–0.91 for k_i = 0.015–0.101 m^{-1}. Consequently, the measured wave attenuation shown in Fig. 3 should have been caused mostly by the artificial seaweed.

For each of the sixty runs, d = 25 cm, b = 5.2 cm, N = 0.110 or 0.149 cm^{-2}, h = 20 or 27 cm, and the values of $f = \omega/(2\pi)$ and H_o are known. The coefficients ϵ and D may be calculated using Eq. 56 where the empirical drag coefficient C_D still needs to be specified. The values of k_r and k_i for each run can then be computed by solving Eq. 28 for $k = (k_r + ik_i)$. The approximate values of k_r and k_i for the case of $\epsilon \ll 1$ can also be computed using Eqs. 31 and 32. Comparison of the measured and computed values of k_r and k_i would indicate the accuracy of the analytical solution presented herein. However, the drag coefficient C_D is uncertain and needs to be calibrated. As a result, the sensitivity of

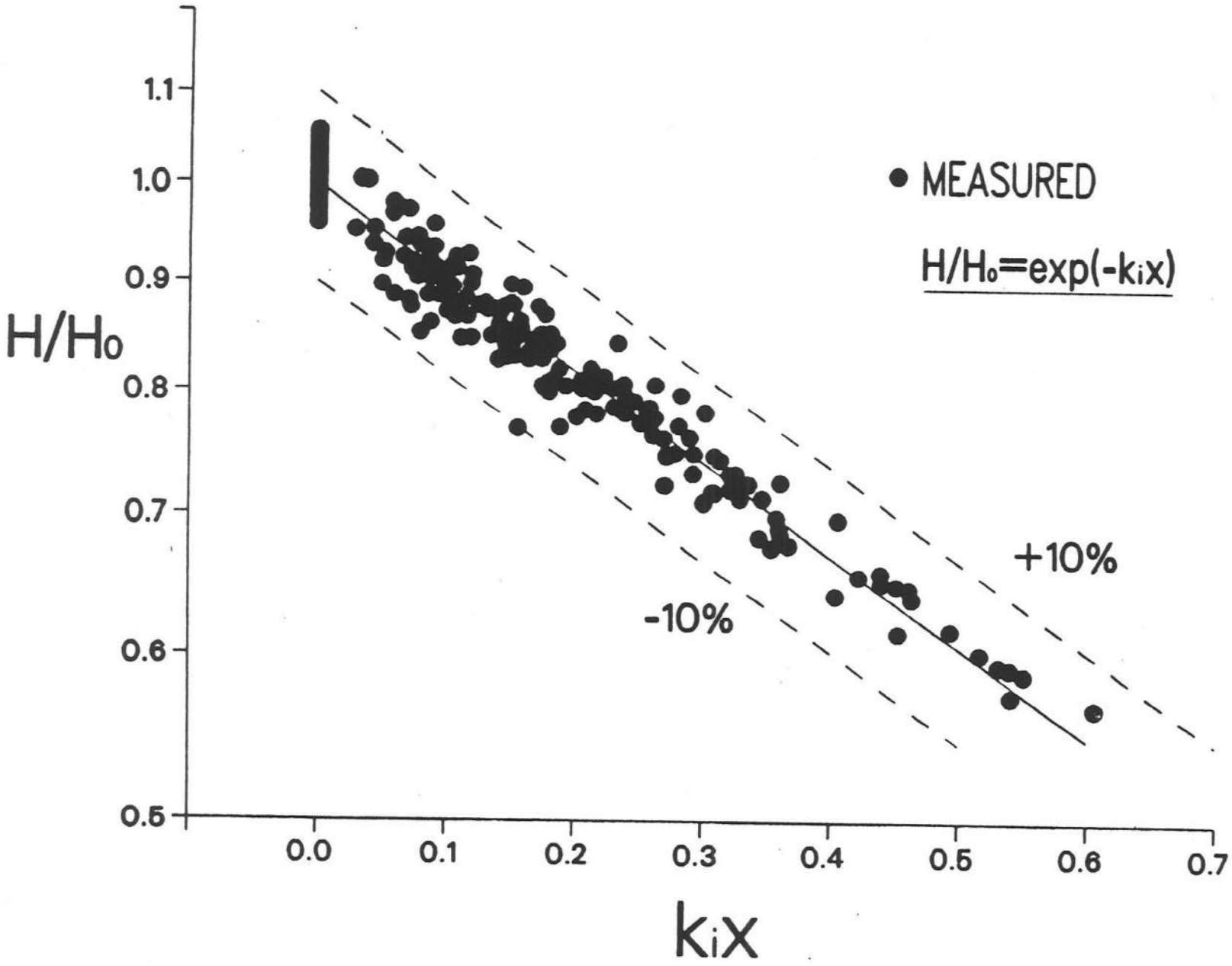

FIG. 3. Measured Wave Heights Fitted to Exponential Decay Model.

the computed values of k_r and k_i is examined first.

The normalized wave number $k_r' = k_r(d+h)$ and the normalized decay coefficient $k_i' = k_i(d+h)$ depend on the dimensionless parameters L_o', d' and ϵ as explained in relation to Eq. 33. For the sixty test runs, $L_o' = 1.5$–13.9, $d' = 0.48$–0.56 and $\epsilon/C_D = 0.053$–0.973 where ϵ given by Eq. 56 is proportional to C_D. Table 3 summarizes the values of the dimensionless parameters for each run. The drag coefficient C_D is expected to be of the order unity or less since C_D is of the order unity for rigid vertical cylinders (e.g., Shore Protection Manual) and the seaweed motion should reduce the drag force as explained in relation to Eq. 10. As a result, use is made of $0 < \epsilon < 1$ in the following computation.

Figs. 4 and 5 show the variations of k_r' and k_i' with respect to ϵ for $d' = 0.5$ and L_o' = 2, 5, 8 and 13, respectively, where k_r' and k_i' are the exact values based on Eq. 28 for arbitrary ϵ. Fig. 4 also shows the ratio of the approximate value of k_r' based on Eq. 31 to the corresponding exact value, while Fig. 5 shows the ratio of the approximate value of k_i' based on Eq. 32 to the corresponding exact value. Fig. 4 indicates that k_r' is not sensitive to ϵ and hence C_D. k_r' increases with the decrease of L_o', which is the normalized wave length in deep water as defined in Eq. 33. The difference between the approximate and exact values of k_r' is small even for large ϵ. Since Eq. 31 is the dispersion relationship based on linear wave theory, the presence of the seaweed slightly increases the wave number and decreases the phase velocity $c = \omega/k_r$. On the other hand, Fig. 5 indicates that k_i' is sensitive to ϵ and hence C_D for small ϵ. The approximate value of k_i' becomes too large relative to the corresponding exact value for large ϵ. The overestimation of k_i' by Eq. 32, which predicts that k_i' is proportional to ϵ, increases as L_o' is increased from 2 to 13. Eq. 32 is applicable only if ϵ is less than approximately 0.1 for $d' = 0.5$ and $L_o' = 2$–13. It is also noted that the variation of k_i' with respect to L_o' is not monotonic for $d' = 0.5$ and $0 < \epsilon < 1$. This variation occurs even for $\epsilon < 0.1$ and may be explained partially using Eqs. 31 and 32. Eqs. 31 and 32 may be simplified for $k_r' \ll 1$ and $k_r' \gg 1$, although the range $L_o' = 2$–13 corresponds to finite water depth. In shallow water with $k_r' \ll 1$, Eq. 31 reduces to $k_r' \simeq (2\pi/L_o')^{1/2}$ and

Table 3: Summary of Dimensionless Parameters for Sixty Test Runs where $\beta = bN\ H_o/2$; $d' = d/(d+h)$; $L'_o = g/[2\pi(d+h)f^2]$; $k'_r = k_r(d+h)$; $k'_i = k_i(d+h)$; and C_D = Calibrated Drag Coefficient. Note that k'_r and k'_i are the measured normalized wave number and decay coefficient, respectively.

Run #	β	d'	Lo'	kr'	ki'	C_D (calibrated)
1	1.39	0.556	13.87	no value	0.0197	0.145
2	4.24	0.556	9.63	1.09	0.0399	0.108
3	2.83	0.556	9.63	1.15	0.0388	0.157
4	5.19	0.556	7.08	1.21	0.0406	0.103
5	3.27	0.556	7.08	1.19	0.0340	0.136
6	5.56	0.556	5.42	1.35	0.0405	0.115
7	3.37	0.556	5.42	no value	0.0316	0.147
8	7.30	0.556	5.42	1.35	0.0414	0.089
9	6.82	0.556	5.42	1.46	0.0455	0.105
10	5.33	0.556	5.42	no value	0.0371	0.109
11	4.56	0.556	5.42	no value	0.0305	0.104
12	4.05	0.556	5.42	no value	0.0348	0.134
13	3.35	0.556	5.42	no value	0.0346	0.162
14	2.80	0.556	5.42	no value	0.0330	0.185
15	1.87	0.556	5.42	no value	0.0252	0.210
16	5.30	0.556	4.28	1.65	0.0330	0.124
17	3.15	0.556	4.28	1.69	0.0260	0.164
18	5.38	0.556	3.47	2.05	0.0209	0.106
19	3.42	0.556	3.47	2.03	0.0175	0.139
20	3.66	0.556	2.41	2.59	0.0134	0.239
21	2.53	0.556	2.41	2.57	0.0168	0.433
22	3.07	0.556	1.77	3.47	0.0160	1.038
23	3.39	0.481	12.01	1.13	0.0281	0.105
24	2.15	0.481	12.01	1.07	0.0218	0.128
25	4.28	0.481	8.34	1.22	0.0246	0.083
26	2.62	0.481	8.34	1.21	0.0203	0.112
27	5.58	0.481	6.13	1.39	0.0272	0.086
28	3.56	0.481	6.13	1.38	0.0251	0.124
29	7.51	0.481	4.69	1.55	0.0313	0.095
30	6.52	0.481	4.69	1.57	0.0279	0.098
31	5.51	0,481	4.69	1.58	0.0236	0.098
32	4.77	0.481	4.69	1.59	0.0236	0.113
33	3.76	0.481	4.69	1.57	0.0206	0.125
34	2.70	0.481	4.69	1.57	0.0184	0.154
35	6.65	0,481	3.71	1.86	0.0227	0.111
36	4.48	0.481	3.71	1.87	0.0228	0.166
37	6.60	0.481	3.00	2.16	0.0178	0.141
38	3.71	0.481	3.00	2.22	0.0153	0.214
39	4.72	0.481	2.08	3.09	0.0163	0.641
40	2.93	0.481	2.08	3.16	0.0087	0.548
41	3.13	0.481	1.53	4.24	0.0101	2.929
42	1.80	0.556	13.87	0.97	0.0164	0.093
43	1.12	0.556	13.87	0.96	0.0113	0.104
44	2.86	0.556	9.63	1.10	0.0339	0.135
45	1.72	0.556	9.63	1.10	0.0245	0.161
46	3.44	0.556	7.08	1.22	0.0269	0.102
47	2.10	0.556	7.08	1.22	0.0180	0.116
48	4.62	0.556	5.42	1.38	0.0241	0.081
49	4.06	0.556	5.42	1.41	0.0232	0.089
50	3.58	0.556	5.42	1.40	0.0193	0.084
51	3.19	0.556	5.42	1.40	0.0244	0.119
52	2.51	0.556	5.42	1.41	0.0194	0.120
53	1.97	0.556	5.42	1.43	0.0165	0.130
54	4.14	0.556	4.28	1.67	0.0202	0.097
55	2.60	0.556	4.28	1.72	0.0185	0.141
56	4.31	0.556	3.47	1.95	0.0118	0.075
57	2.49	0.556	3.47	1.98	0.0100	0.109
58	3.26	0.556	2.41	2.74	0.0115	0.229
59	1.74	0.556	2.41	2.74	0.0066	0.247
60	1.95	0.556	1.77	3.57	0.0098	0.992

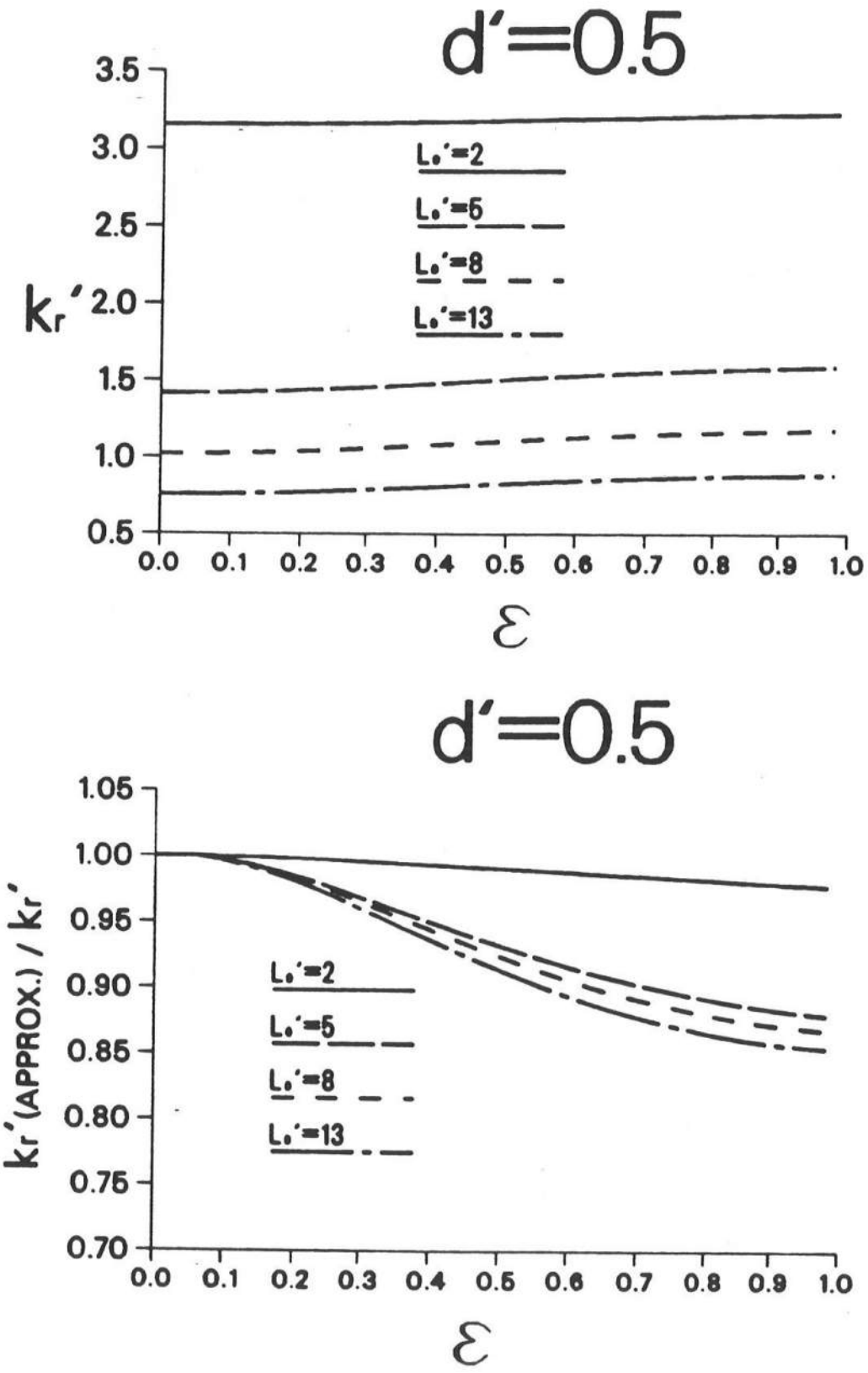

FIG. 4. Normalized Wave Number k_r' and Ratio between Approximate and Exact Values of k_r' as a Function of ϵ for $d' = 0.5$ and $L_o' = 2$, 5, 8 and 13.

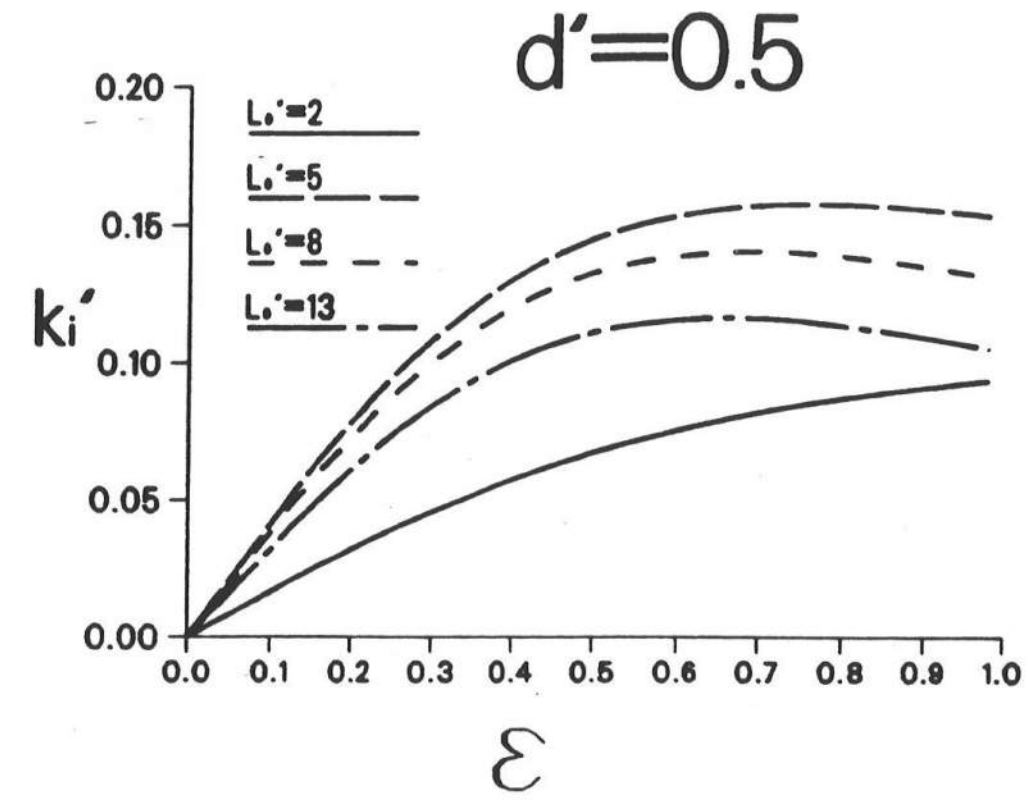

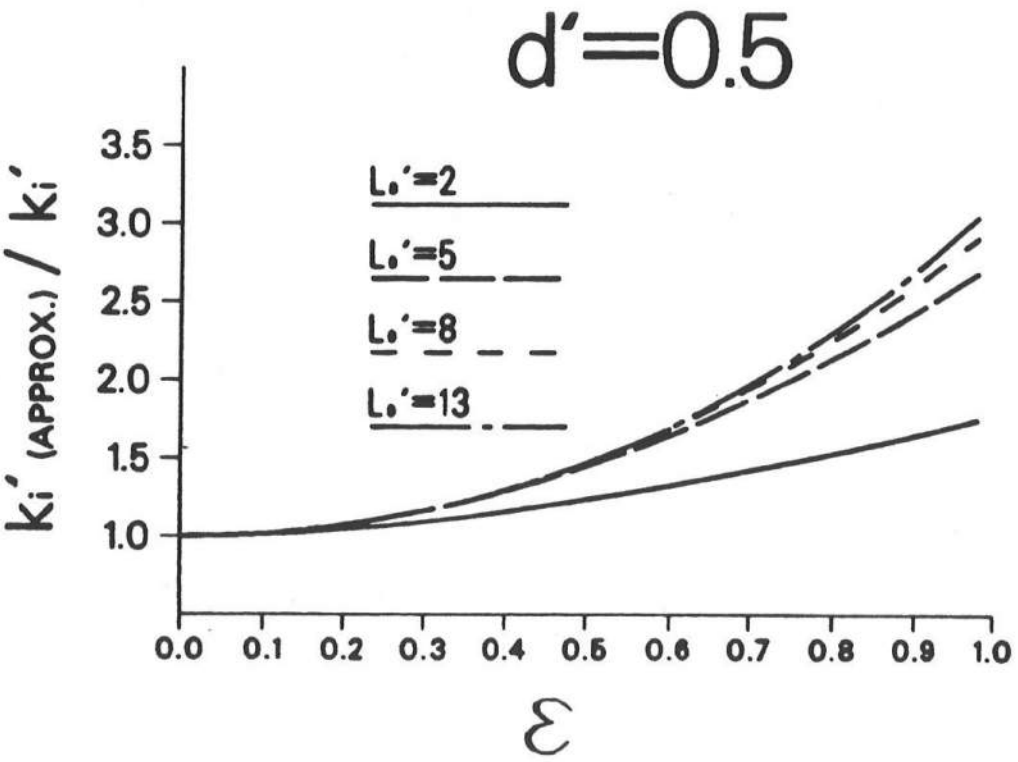

FIG. 5. Normalized Decay Coefficient k_i' and Ratio between Approximate and Exact Values of k_i' as a Function of ϵ for $d' = 0.5$ and $L_o' = 2$, 5, 8 and 13.

Eq. 32 may be approximated by

$$k_i' \simeq \epsilon d' \left(\frac{2\pi}{L_o'}\right)^{1/2} \tag{57}$$

Eq. 57 implies that long waves are attenuated less by the seaweed. On the other hand, in deep water with $k_r' \gg 1$, Eq. 31 reduces to $k_r' \simeq 2\pi/L_o'$ and Eq. 32 may be approximated as

$$k_i' \simeq \epsilon \frac{2\pi}{L_o'} \exp\left[-\frac{4\pi}{L_o'}(1-d')\right] \tag{58}$$

where $d' = d/(h+d)$ is assumed to be of the order unity. In deep water, k_i' increases and then decreases as L_o' is increased. The maximum value of k_i' occurs at $L_o' = 4\pi(1-d')$, which yields $L_o' = 2\pi$ for $d' = 0.5$. The variation of k_i' with respect to L_o' shown in Fig. 5 is qualitatively similar to that based on Eq. 58, although Eq. 58 is appropriate only for $\epsilon \ll 1$ and in deep water.

In view of the computed results shown in Figs. 4 and 5, the calibrated value of C_D for each run is obtained such that the exact value of k_i' computed from Eq. 28 equals the measured value of k_i' for each run. The bisection method (e.g., Press et al. 1986) is used to compute the calibrated value of C_D for each run. The calibrated values of C_D for the sixty runs are listed in Table 3 and vary in the wide range 0.075–2.93. The corresponding values of ϵ are in the smaller range 0.021–0.156. The differences between the exact and approximate values of k_i' and k_r' are less than 2.0% and 0.4%, respectively. As a result, the approximate expressions given by Eqs. 31 and 32 turn out to be very accurate for the sixty runs as shown in Table 4.

In order to find possible explanations for the large variation of C_D, the calibrated values of C_D are plotted as a function of the Reynolds number, Re, defined as $Re = b\, u_c/\nu$ in which b = width of the seaweed; ν = kinematic viscosity of the water; and u_c = characteristic fluid velocity acting on the seaweed defined as

$$u_c = \frac{k_r\, g\, H_o}{2\omega} \frac{\cosh(k_r\, d)}{\cosh[k_r(h+d)]} \tag{59}$$

where k_r is computed using Eq. 31. u_c given by Eq. 59 is the maximum value of the horizontal velocity u_1 at $x = 0$ and $z = -h$ obtained from Eqs. 20 and 43 with $c_1 = 0$, corresponding to linear wave theory. Fig. 6 shows the calibrated values of C_D as a function

Table 4: Approximate and Exact Values of k_r' and k_i' Together with Difference $e_r(\%)$ Defined as e_r = 100 (Approximate Value–Exact Value)/(Exact Value) for Calibrated C_D.

Run #	ε	kr'		e_r (%)	ki'		e_r (%)
		approx	exact		approx	exact	
1	0.055	0.729	0.730	-0.137	0.0198	0.0197	0.508
2	0.098	0.908	0.911	-0.329	0.0406	0.0399	1.740
3	0.095	0.908	0.911	-0.329	0.0394	0.0388	1.546
4	0.090	1.108	1.110	-0.180	0.0414	0.0406	1.970
5	0.075	1.108	1.109	0.000	0.0344	0.0340	1.176
6	0.085	1.333	1.337	-0.299	0.0413	0.0405	1.975
7	0.066	1.333	1.335	-0.150	0.0320	0.0317	0.095
8	0.087	1.333	1.337	-0.299	0.0420	0.0414	1.449
9	0.095	1.333	1.338	-0.374	0.0462	0.0455	1.538
10	0.077	1.333	1.336	-0.225	0.0375	0.0371	1.078
11	0.063	1.333	1.335	-0.150	0.0306	0.0305	0.328
12	0.072	1.333	1.336	-0.225	0.0350	0.0348	0.575
13	0.072	1.333	1.336	-0.225	0.0350	0.0346	1.156
14	0.069	1.333	1.336	-0.225	0.0334	0.0330	1.212
15	0.052	1.333	1.334	-0.075	0.0254	0.0252	0.794
16	0.069	1.593	1.597	-0.250	0.0332	0.0330	0.606
17	0.054	1.593	1.596	-0.188	0.0261	0.0260	0.385
18	0.047	1.895	1.896	-0.053	0.0210	0.0209	0.478
19	0.039	1.895	1.895	0.000	0.0175	0.0175	0.000
20	0.043	2.636	2.635	0.000	0.0135	0.0134	0.746
21	0.054	2.636	2.635	0.000	0.0170	0.0168	1.190
22	0.094	3.557	3.557	0.000	0.0163	0.0160	1.875
23	0.088	0.794	0.796	-0.251	0.0285	0.0281	1.423
24	0.068	0.794	0.794	0.000	0.0220	0.0218	0.917
25	0.067	0.996	0.995	0.001	0.0248	0.0246	0.813
26	0.055	0.996	0.995	0.001	0.0205	0.0203	0.985
27	0.070	1.223	1.223	0.000	0.0276	0.0272	1.471
28	0.064	1.223	1.223	0.000	0.0254	0.0251	1.195
29	0.079	1.484	1.488	-0.269	0.0316	0.0313	0.958
30	0.071	1.484	1.487	-0.202	0.0283	0.0279	1.434
31	0.060	1.484	1.487	-0.202	0.0239	0.0236	1.271
32	0.060	1.484	1.487	-0.202	0.0239	0.0236	1.271
33	0.052	1.484	1.486	-0.135	0.0208	0.0206	0.971
34	0.046	1.484	1.486	-0.135	0.0184	0.0184	0.000
35	0.062	1.792	1.792	0.000	0.0229	0.0227	0.881
36	0.062	1.792	1.792	0.000	0.0230	0.0228	0.877
37	0.058	2.151	2.153	-0.093	0.0180	0.0178	1.111
38	0.049	2.151	2.153	-0.093	0.0153	0.0153	0.000
39	0.099	3.029	3.035	-0.198	0.0164	0.0163	0.613
40	0.052	3.029	3.035	-0.198	0.0087	0.0087	0.000
41	0.156	4.105	4.106	0.000	0.0103	0.0101	1.980
42	0.046	0.729	0.729	0.000	0.0164	0.0164	0.000
43	0.032	0.729	0.729	0.000	0.0114	0.0113	0.885
44	0.082	0.908	0.910	-0.220	0.0343	0.0339	1.180
45	0.059	0.908	0.908	0.000	0.0246	0.0245	0.408
46	0.059	1.108	1.108	0.000	0.0272	0.0269	1.115
47	0.039	1.108	1.107	0.090	0.0181	0.0180	0.556
48	0.050	1.333	1.334	-0.075	0.0242	0.0241	0.415
49	0.048	1.333	1.334	-0.075	0.0233	0.0232	0.431
50	0.040	1.333	1.334	-0.075	0.0194	0.0193	0.518
51	0.051	1.333	1.334	-0.075	0.0245	0.0244	0.410
52	0.040	1.333	1.334	-0.075	0.0194	0.0194	0.000
53	0.034	1.333	1.333	0.000	0.0165	0.0165	0.000
54	0.042	1.593	1.595	-0.125	0.0203	0.0202	0.495
55	0.038	1.593	1.595	-0.125	0.0185	0.0185	0.000
56	0.026	1.895	1.895	0.000	0.0119	0.0118	0.847
57	0.022	1.895	1.895	0.000	0.0101	0.0100	1.000
58	0.037	2.636	2.635	0.000	0.0115	0.0115	0.000
59	0.021	2.636	2.634	0.001	0.0066	0.0066	0.000
60	0.057	3.557	3.556	0.000	0.0099	0.0098	1.020

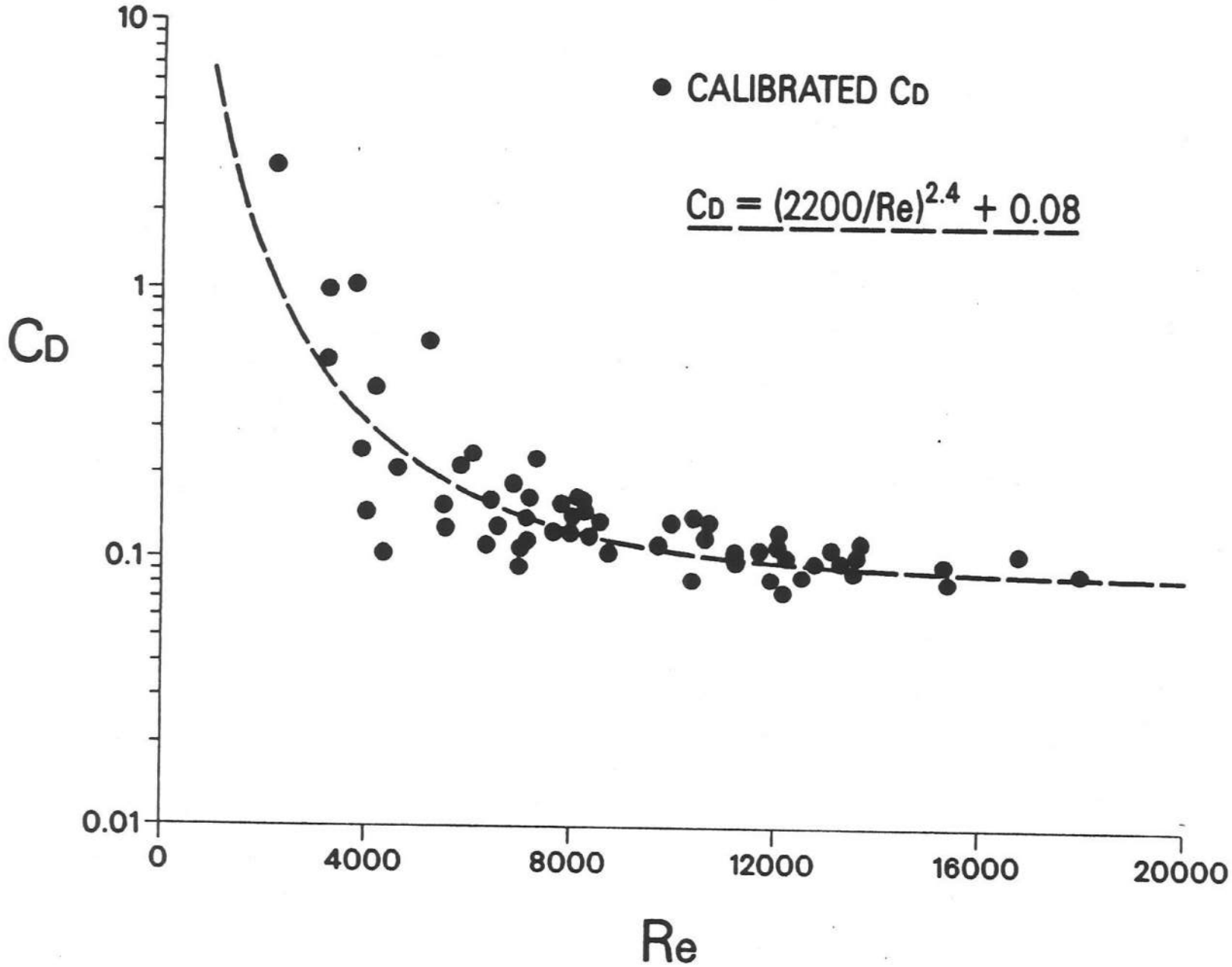

FIG. 6. Calibrated Values of Drag Coefficient C_D as a Function of Reynolds Number Re.

of Re for the sixty runs for which $b = 5.2$ cm, $\nu \simeq 0.01$ cm^2/s and $u_c = 4.3$–34.6 cm/s. Fig. 6 indicates that C_D tends to decrease with the increase of Re and is of the order 0.1 for large Re. The data points in Fig. 6 may be represented by the following empirical relationship between C_D and Re for $2200 < \mathrm{Re} < 18000$.

$$C_D = \left(\frac{2200}{Re}\right)^{2.4} + 0.08 \tag{60}$$

The decrease of C_D with the increase of Re may be explained partly by the skin friction on the surface of the seaweed which may be affected by the viscous effects. Eq. 60 also implies that C_D decreases with the increase of u_c since $b = 5.2$ cm and $\nu \simeq 0.01$ cm^2/s for these test runs. The decrease of C_D with the increase of u_c may be explained partly by the increase of the bending motion of the seaweed with the increase of u_c. The use of the horizontal fluid velocity relative to the horizontal seaweed velocity is expected to reduce the variation of C_D with u_c. Table 5 lists the calibrated value of C_D as compared to the empirical value of C_D based on Eq. 60 for each of the sixty runs.

Finally, the normalized wave number k_r' and the normalized decay coefficient k_i' for each of the sixty runs are computed using Eqs. 27, 28 and 56 with C_D being estimated by Eq. 60 as listed in Table 6. The computed values using the approximate expressions given by Eqs. 31 and 32 are essentially the same as shown in Table 7. Figs. 7 and 8 show the comparison between the measured and computed values of k_r' and k_i', respectively. Fig. 7 implies that the dispersion relationship based on linear wave theory is applicable for these test runs. The slight underestimation of k_r' by the analytical solution for small k_r' may be related to the difficulty in measuring the small travel time of the wave crests accurately when the phase velocity $c = \omega/k_r$ is large. On the other hand, Fig. 8 indicates that the agreement between the measured and computed values of k_i' is not very good although Eq. 60 is developed using the same data set. Improvement of the empirical relationship for C_D will result in better agreement in Fig. 8. However, the empirical relationship for C_D developed using the present data set may possibly be limited to the specific artificial seaweed used in this experiment.

Table 5: Calibrated and Empirical Values of Drag Coefficient C_D Together with Characteristic Fluid Velocity u_c and Reynolds Number Re for Each of Sixty Test Runs.

Run #	Uc (cm/s)	Re	C_D (calibrated)	C_D (empirical)
1	7.7	4012	0.145	0.316
2	22.5	11702	0.108	0.098
3	15.0	7821	0.157	0.128
4	26.2	13603	0.103	0.093
5	16.5	8576	0.136	0.118
6	26.3	13673	0.115	0.092
7	15.9	8284	0.147	0.122
8	34.6	17976	0.089	0.086
9	32.3	16775	0.105	0.088
10	25.2	13109	0.109	0.094
11	21.6	11218	0.104	0.100
12	19.2	9978	0.134	0.107
13	15.9	8249	0.162	0.122
14	13.2	6884	0.185	0.145
15	8.9	4613	0.210	0.249
16	23.2	12078	0.124	0.097
17	13.8	7192	0.164	0.138
18	21.6	11219	0.106	0.100
19	13.7	7138	0.139	0.139
20	11.7	6086	0.239	0.167
21	8.1	4193	0.433	0.293
22	7.3	3806	1.038	0.348
23	16.8	8746	0.105	0.116
24	10.7	5556	0.128	0.188
25	20.0	10382	0.083	0.104
26	12.2	6358	0.112	0.158
27	24.1	12532	0.086	0.095
28	15.4	7998	0.124	0.125
29	29.4	15310	0.095	0.090
30	25.6	13290	0.098	0.093
31	21.6	11234	0.097	0.100
32	18.7	9723	0.113	0.108
33	14.7	7667	0.125	0.130
34	10.6	5516	0.154	0.190
35	23.2	12055	0.111	0.097
36	15.6	8134	0.166	0.123
37	20.0	10407	0.141	0.104
38	11.3	5852	0.214	0.176
39	10.1	5241	0.641	0.205
40	6.3	3252	0.548	0.471
41	4.3	2233	2.929	1.045
42	13.5	6997	0.093	0.142
43	8.4	4346	0.104	0.275
44	20.6	10710	0.135	0.102
45	12.4	6439	0.161	0.156
46	23.5	12224	0.102	0.096
47	13.8	7153	0.116	0.139
48	29.6	15393	0.081	0.089
49	26.0	13540	0.089	0.093
50	22.9	11922	0.084	0.097
51	20.4	10633	0.119	0.103
52	16.1	8369	0.120	0.121
53	12.6	6577	0.130	0.152
54	24.6	12799	0.097	0.095
55	15.5	8039	0.141	0.125
56	23.4	12165	0.075	0.097
57	13.5	7024	0.109	0.142
58	14.1	7330	0.229	0.136
59	7.5	3914	0.247	0.331
60	6.3	3276	0.992	0.465

Table 6: Computed Exact Values of k_r' and k_i' Using Empirical Value of C_D as Compared with Measured Values of k_r' and k_i' for Each Run.

Run #	C_D (empirical)	ε	kr'		ki'	
			computed	measured	computed	measured
1	0.316	0.121	0.734	no value	0.0422	0.0197
2	0.098	0.089	0.910	1.094	0.0364	0.0399
3	0.128	0.077	0.910	1.146	0.0317	0.0388
4	0.093	0.081	1.110	1.214	0.0367	0.0406
5	0.118	0.065	1.108	1.185	0.0297	0.0340
6	0.092	0.068	1.336	1.354	0.0329	0.0405
7	0.122	0.054	1.335	no value	0.0262	0.0317
8	0.086	0.084	1.337	1.354	0.0402	0.0414
9	0.088	0.080	1.337	1.459	0.0381	0.0455
10	0.094	0.067	1.335	no value	0.0320	0.0371
11	0.100	0.061	1.335	no value	0.0292	0.0305
12	0.107	0.058	1.335	no value	0.0277	0.0348
13	0.122	0.054	1.335	no value	0.0262	0.0346
14	0.145	0.054	1.335	no value	0.0260	0.0330
15	0.249	0.062	1.335	no value	0.0299	0.0252
16	0.097	0.054	1.595	1.652	0.0258	0.0330
17	0.138	0.046	1.595	1.685	0.0219	0.0260
18	0.100	0.044	1.896	2.049	0.0197	0.0209
19	0.139	0.039	1.896	2.034	0.0175	0.0175
20	0.167	0.030	2.636	2.590	0.0094	0.0134
21	0.293	0.036	2.636	2.570	0.0114	0.0168
22	0.348	0.032	3.557	3.472	0.0054	0.0160
23	0.116	0.098	0.797	1.134	0.0310	0.0281
24	0.188	0.100	0.797	1.075	0.0318	0.0218
25	0.104	0.084	0.997	1.218	0.0306	0.0246
26	0.158	0.078	0.996	1.210	0.0285	0.0203
27	0.095	0.077	1.224	1.396	0.0303	0.0272
28	0.125	0.065	1.223	1.378	0.0254	0.0251
29	0.090	0.075	1.488	1.547	0.0294	0.0313
30	0.093	0.068	1.487	1.565	0.0267	0.0279
31	0.100	0.061	1.487	1.584	0.0242	0.0236
32	0.108	0.058	1.486	1.594	0.0227	0.0236
33	0.130	0.054	1.486	1.565	0.0215	0.0206
34	0.190	0.057	1.486	1.575	0.0226	0.0184
35	0.097	0.054	1.794	1.861	0.0198	0.0227
36	0.123	0.046	1.793	1.873	0.0170	0.0228
37	0.104	0.043	2.152	2.164	0.0132	0.0178
38	0.176	0.040	2.152	2.223	0.0126	0.0153
39	0.205	0.032	3.029	3.087	0.0053	0.0163
40	0.471	0.045	3.029	3.162	0.0075	0.0087
41	1.045	0.056	4.106	4.235	0.0037	0.0101
42	0.142	0.070	0.730	0.975	0.0248	0.0164
43	0.275	0.084	0.731	0.962	0.0297	0.0113
44	0.102	0.063	0.909	1.102	0.0258	0.0339
45	0.156	0.057	0.908	1.102	0.0237	0.0245
46	0.096	0.056	1.108	1.222	0.0255	0.0269
47	0.139	0.047	1.107	1.222	0.0216	0.0180
48	0.089	0.055	1.335	1.379	0.0265	0.0241
49	0.093	0.050	1.334	1.414	0.0242	0.0232
50	0.097	0.046	1.334	1.396	0.0224	0.0193
51	0.103	0.044	1.334	1.396	0.0211	0.0244
52	0.121	0.040	1.334	1.414	0.0195	0.0194
53	0.152	0.040	1.334	1.432	0.0193	0.0165
54	0.095	0.041	1.595	1.674	0.0197	0.0202
55	0.125	0.034	1.594	1.719	0.0163	0.0185
56	0.097	0.034	1.896	1.950	0.0152	0.0118
57	0.142	0.029	1.896	1.977	0.0129	0.0100
58	0.136	0.022	2.636	2.736	0.0068	0.0115
59	0.331	0.028	2.636	2.736	0.0089	0.0066
60	0.465	0.027	3.557	3.566	0.0046	0.0098

Table 7: Approximate and Exact Values of k_r' and k_i' Together with Difference $e_r(\%)$ Defined as e_r = 100 (Approximate Value–Exact Value)/(Exact Value) for Empirical C_D.

Run #	kr'		e_r	ki'		e_r
	approx	exact	(%)	approx	exact	(%)
1	0.729	0.734	-0.681	0.0433	0.0422	2.607
2	0.908	0.910	-0.220	0.0369	0.0364	1.374
3	0.908	0.910	-0.220	0.0321	0.0317	1.262
4	1.108	1.110	-0.180	0.0372	0.0367	1.362
5	1.108	1.108	0.000	0.0299	0.0297	0.673
6	1.333	1.336	-0.225	0.0331	0.0329	0.608
7	1.333	1.335	-0.150	0.0264	0.0262	0.763
8	1.333	1.337	-0.299	0.0407	0.0402	1.244
9	1.333	1.337	-0.299	0.0385	0.0381	1.050
10	1.333	1.335	-0.150	0.0322	0.0320	0.625
11	1.333	1.335	-0.150	0.0294	0.0292	0.685
12	1.333	1.335	-0.150	0.0279	0.0277	0.722
13	1.333	1.335	-0.150	0.0264	0.0262	0.763
14	1.333	1.335	-0.150	0.0261	0.0260	0.385
15	1.333	1.335	-0.150	0.0301	0.0299	0.669
16	1.593	1.595	-0.125	0.0259	0.0258	0.388
17	1.593	1.595	-0.125	0.0220	0.0219	0.457
18	1.895	1.896	-0.053	0.0198	0.0197	0.508
19	1.895	1.896	-0.053	0.0175	0.0175	0.000
20	2.636	2.636	0.000	0.0094	0.0094	0.000
21	2.636	2.636	0.000	0.0114	0.0114	0.000
22	3.557	3.557	0.000	0.0054	0.0054	0.000
23	0.794	0.797	-0.376	0.0316	0.0310	1.935
24	0.794	0.797	-0.376	0.0324	0.0318	1.887
25	0.996	0.997	-0.100	0.0310	0.0306	1.307
26	0.996	0.996	0.000	0.0289	0.0285	1.404
27	1.223	1.224	-0.082	0.0306	0.0303	0.990
28	1.223	1.223	0.000	0.0256	0.0254	0.787
29	1.484	1.488	-0.269	0.0297	0.0294	1.020
30	1.484	1.487	-0.202	0.0269	0.0267	0.749
31	1.484	1.487	-0.202	0.0244	0.0242	0.826
32	1.484	1.486	-0.135	0.0228	0.0227	0.441
33	1.484	1.486	-0.135	0.0216	0.0215	0.465
34	1.484	1.486	-0.135	0.0228	0.0226	0.885
35	1.792	1.794	-0.111	0.0199	0.0198	0.505
36	1.792	1.793	-0.056	0.0171	0.0170	0.588
37	2.151	2.152	-0.046	0.0133	0.0132	0.758
38	2.151	2.152	-0.046	0.0126	0.0126	0.000
39	3.029	3.029	0.000	0.0053	0.0053	0.000
40	3.029	3.029	0.000	0.0075	0.0075	0.000
41	4.105	4.106	-0.024	0.0037	0.0037	0.000
42	0.729	0.730	-0.137	0.0250	0.0248	0.806
43	0.729	0.731	-0.274	0.0301	0.0297	1.347
44	0.908	0.909	-0.110	0.0260	0.0258	0.775
45	0.908	0.908	0.000	0.0238	0.0237	0.422
46	1.108	1.108	0.000	0.0256	0.0255	0.392
47	1.108	1.107	0.090	0.0217	0.0216	0.463
48	1.333	1.335	-0.150	0.0266	0.0265	0.377
49	1.333	1.334	-0.075	0.0243	0.0242	0.413
50	1.333	1.334	-0.075	0.0224	0.0224	0.000
51	1.333	1.334	-0.075	0.0211	0.0211	0.000
52	1.333	1.334	-0.075	0.0195	0.0195	0.000
53	1.333	1.334	-0.075	0.0194	0.0193	0.518
54	1.593	1.595	-0.125	0.0198	0.0197	0.508
55	1.593	1.594	-0.063	0.0164	0.0163	0.614
56	1.895	1.896	-0.053	0.0153	0.0152	0.658
57	1.895	1.896	-0.053	0.0129	0.0129	0.000
58	2.636	2.636	0.000	0.0068	0.0068	0.000
59	2.636	2.636	0.000	0.0089	0.0089	0.000
60	3.557	3.557	0.000	0.0046	0.0046	0.000

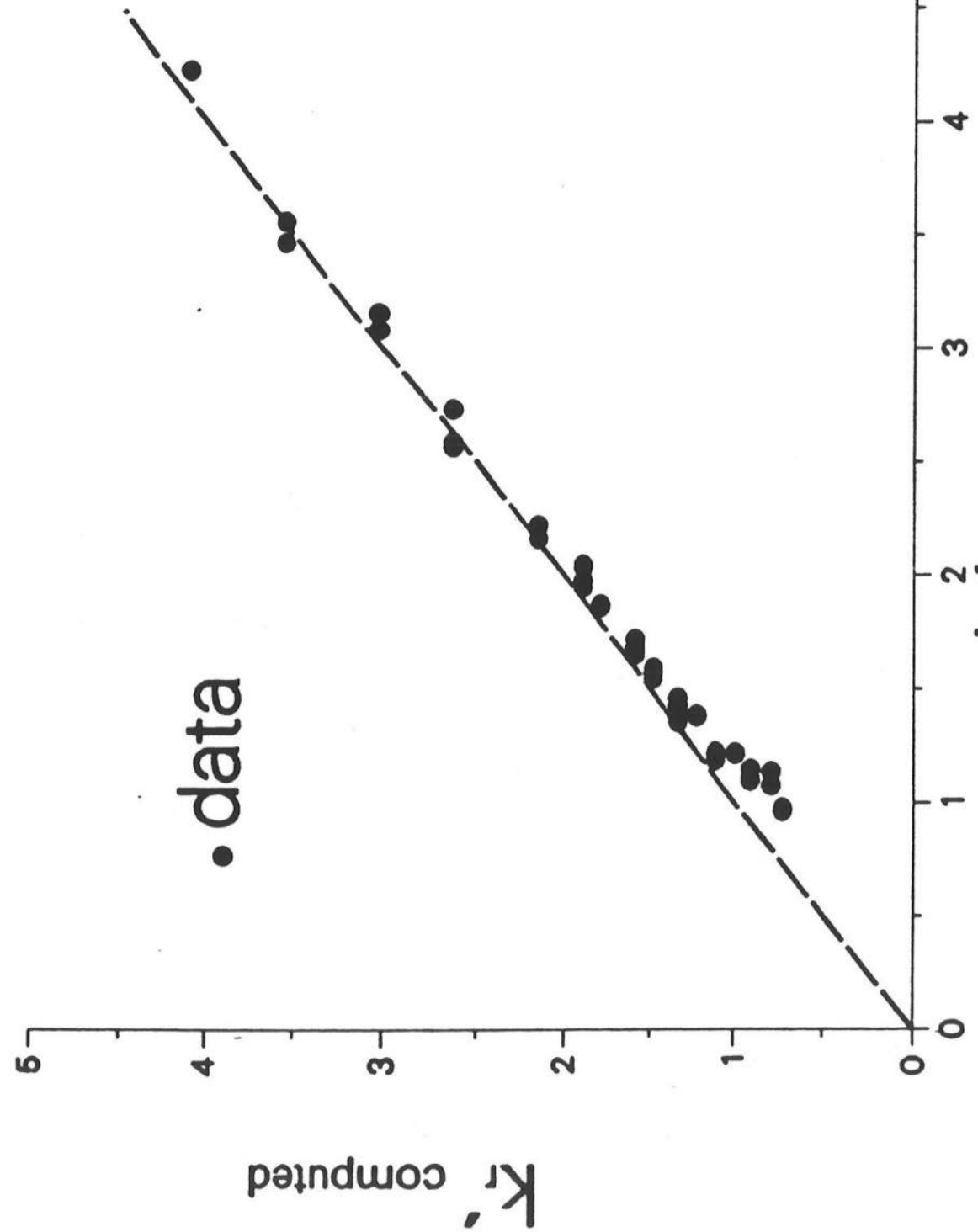

FIG. 7. Comparison between Measured and Computed Values of Normalized Wave Number k_r'.

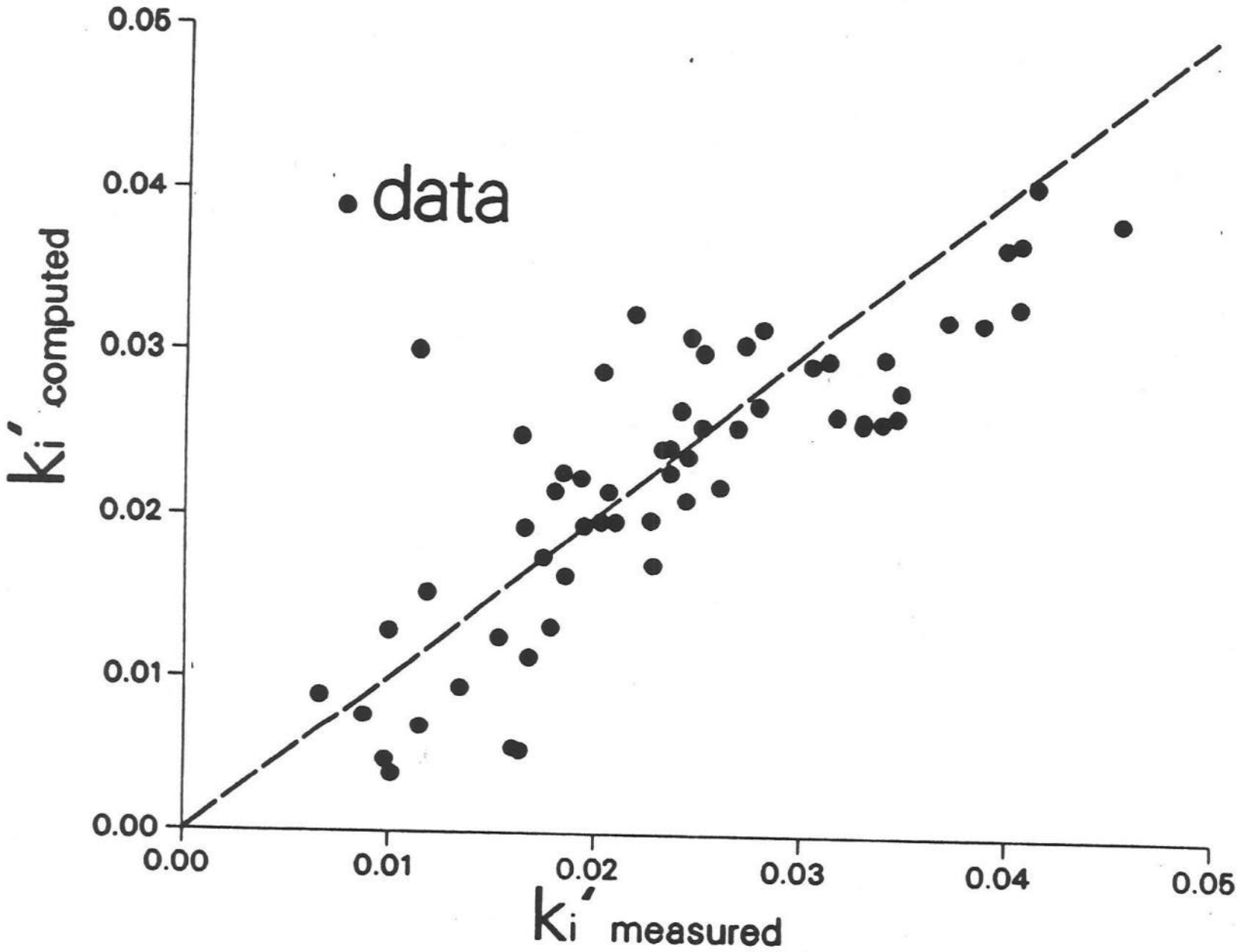

FIG. 8. Comparison between Measured and Computed Values of Normalized Decay Coefficient k_i'.

WAVE ATTENUATION BY SUBAERIAL VEGETATION

The analytical solution presented herein is also applicable to subaerial vegetation for which $h = 0$ and d is the water depth. For $h = 0$, the conditions at the interface $z = -h$ given by Eqs. 12, 13 and 14 ensure that the free surface boundary conditions given by Eqs. 4 and 5 are satisfied by the solution for the vegetated region. Comparison of Eq. 23 with $h = 0$ with Eq. 19 shows that $\eta_2 = \eta_1$ for $h = 0$. Eq. 26 with $h = 0$ satisfies the dynamic boundary condition, $p_2 = \rho g \eta_2$ at $z = 0$. Eqs. 25 and 26 with $h = 0$ can be shown to satisfy the kinematic boundary condition, $w_2 = \partial \eta_2 / \partial t$ at $z = 0$, where η_2 is given by Eq. 23 with $h = 0$ and Eq. 28 with $h = 0$ reduces to

$$\omega^2 = \alpha g \tanh(\alpha d) \tag{61}$$

in which α is defined by Eq. 27. Furthermore, Eqs. 31 and 32 for the case of $\epsilon \ll 1$ can be simplified as

$$\omega^2 \simeq k_r g \tanh(k_r d) \tag{62}$$

$$k_i \simeq \epsilon k_r \tag{63}$$

For the case of subaerial vegetation, the normalized wave number, $k'_r = k_r d$, and the normalized decay coefficient, $k'_i = k_i d$, depend on the normalized deep water wavelength, $L'_o = 2\pi g/(d\omega^2)$, and the dimensionless damping coefficient ϵ which may be estimated using Eq. 56 with $h = 0$. In short, the analytical solution obtained for arbitrary $h \geq 0$ can be used to examine the wave attenuation for the case of $h = 0$ and hence $d' = d/(h + d) = 1$ in Eq. 33.

Figs. 9 and 10 show the computed variations of k'_r and k'_i with respect to ϵ in the range $0 < \epsilon < 1$ for $L'_o = 2$, 10 and 90, respectively, where k'_r and k'_i are the exact values based on Eq. 61 for arbitrary ϵ. Fig. 9 also shows the ratio of the approximate value of k'_r based on Eq. 62 to the corresponding exact value, while Fig. 10 shows the ratio of the approximate value of k'_i based on Eq. 63 to the corresponding exact value. Comparison of Figs. 9 and 10 with

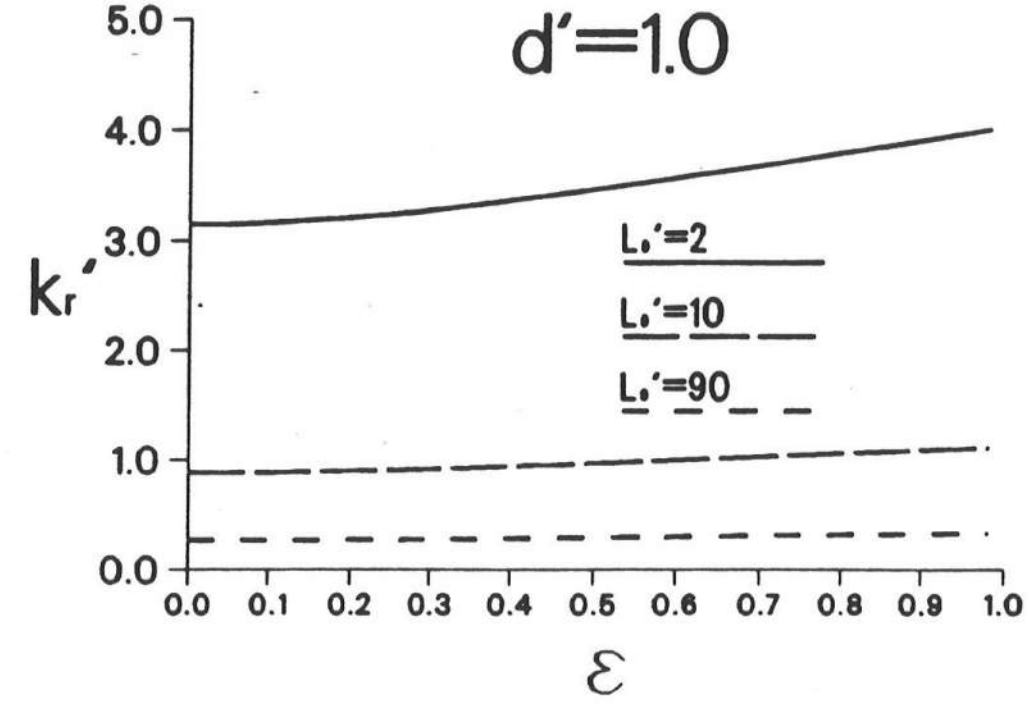

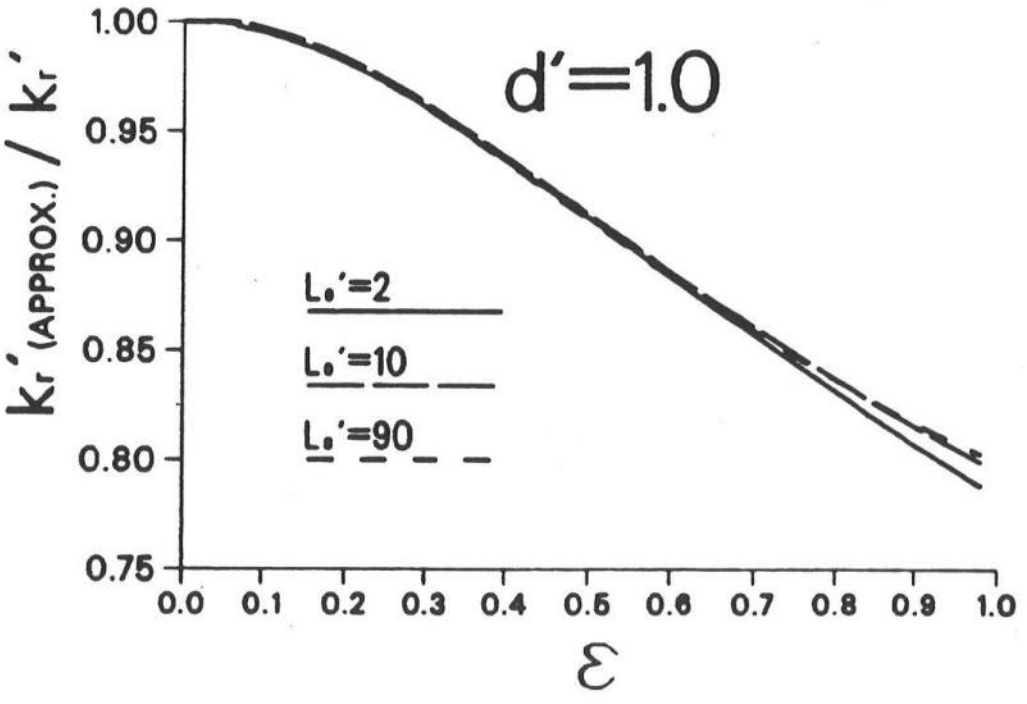

FIG. 9. Normalized Wave Number k_r' and Ratio between Approximate and Exact Values of k_r' as a Function of ϵ with L_o' = 2, 10 and 90 for Subaerial Vegetation.

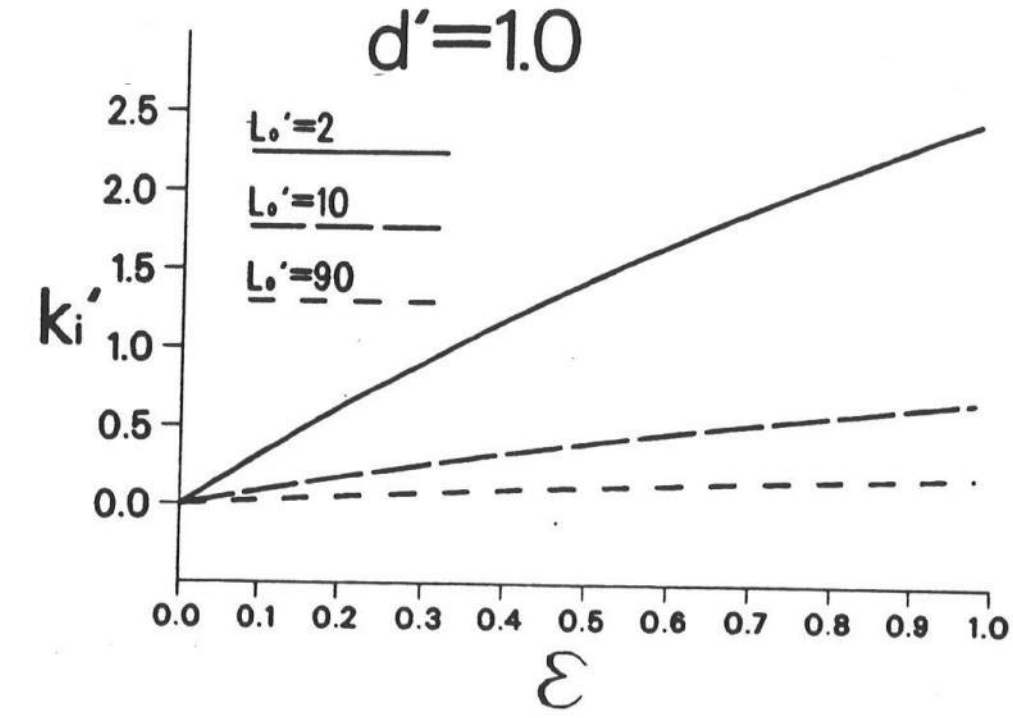

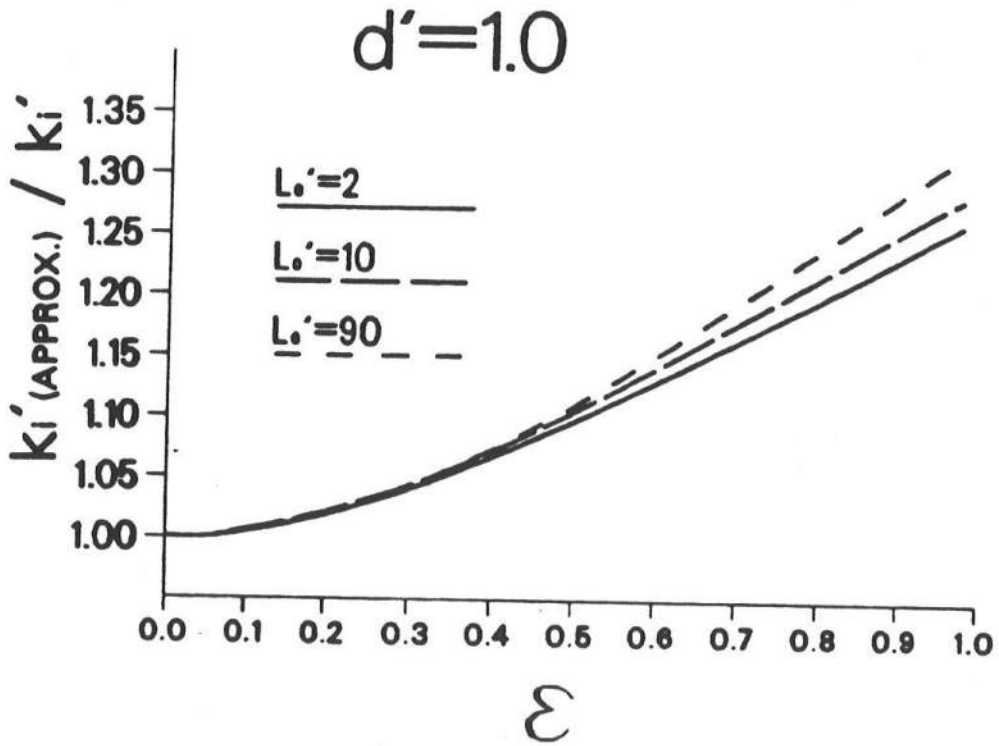

FIG. 10. Normalized Decay Coefficient k_i' and Ratio between Approximate and Exact Values of k_i' as a Function of ϵ with $L_o' = 2$, 10 and 90 for Subaerial Vegetation.

Figs. 4 and 5 indicates the sensitivity of the computed results to the dimensionless parameter d'. Fig. 9 indicates that k_r' is not sensitive to ϵ even for $d' = 1$. The difference between the approximate and exact values of k_r' is not very large even for large ϵ. The increase of d' from 0.5 results in a slight decrease of the phase velocity c. Fig. 10 shows that the difference between the approximate and exact values of k_i' is reduced for $d' = 1$ as compared to Fig. 5 for $d' = 0.5$. Accordingly, the exact value of k_i' increases approximately linearly with the increase in ϵ where the approximate value of k_i' based on Eq. 63 is proportional to ϵ. Fig. 10 for $d' = 1$ indicates the monotonic decrease of k_i' with the increase of L_o' unlike Fig. 5 for $d' = 0.5$. This can be shown using Eqs. 62 and 63 for small ϵ and using Eqs. 57 and 58 with $d' = 1$. Moreover, comparison of Figs. 5 and 10 suggests that k_i' increases significantly with the increase of d' from 0.5 to 1.0. Consequently, subaerial vegetation will be much more effective in dissipating wave energy than deeply submerged vegetation.

SUMMARY AND CONCLUSIONS

The vertically two-dimensional problem of small-amplitude waves propagating over submerged vegetation without lateral boundaries has been formulated using the continuity and linearized momentum equations for the regions with and without the vegetation. The effects of the vegetation on the flow field have been assumed to be expressible in terms of the drag force acting on the vegetation. Introducing an unknown damping coefficient and linearizing the drag force, an analytical solution has been obtained for the small-amplitude monochromatic wave whose height decays exponentially in the direction of wave propagation. The unknown damping coefficient has been obtained such that the nonlinear and linearized drag forces yield approximately the same time-averaged rate of energy dissipation in the vegetated region. The expressions for the wave number and the exponential decay coefficient have been derived for arbitrary damping. It has been shown for the case of small damping that the wave number approaches that based on the dispersion relationship of linear wave theory without damping, whereas the exponential decay coefficient approaches that based on the standard conservation equation of energy based on linear wave theory. However, the

local flow field has been shown to be affected by the vegetation even for the case of small damping. This may be important for analyses of phenomena affected by the local flow field, such as sediment transport in vegetated areas.

The analytical solution derived herein has been compared with the artificial seaweed experiment conducted by Asano et al. (1988). The measured local wave heights for the sixty test runs have been shown to follow the exponentially decay fairly well. The drag coefficient used to express the drag force acting on the vegetation has been calibrated using the exponential decay coefficient fitted for each run. The assumption of small damping has been found to be appropriate for these runs. The calibrated drag coefficients have turned out to vary in a wide range and appear to have been affected by the seaweed motion and viscous effects, which are neglected in the present analysis. Finally, the analytical solution derived for submerged vegetation has been shown to be applicable to subaerial vegetation as well. The analytical results have indicated that subaerial vegetation will be much more effective in dissipating wave energy than deeply submerged vegetation.

In conclusion, the standard simple approach based on the conservation equation of energy and linear wave theory appears to be acceptable in predicting the decay of the local wave height for most practical applications. The analytical solution presented herein can be used to quantify the error caused by the assumption of small damping. Extensive field data will be required to better predict the drag coefficient for different types of vegetation. Moreover, the standard approach and the present analysis will need to be extended to wind waves.

REFERENCES

Asano, T., Tsutsui, S. and Sakai, T. (1988). "Wave damping characteristics due to seaweed." *Proc. 35th Coast. Engrg. Conf. in Japan*, 138–142 (in Japanese).

ASCE Task Committee on sea level rise and its effects on bays and estuaries (1992). "Effects of sea level rise on bays and estuaries." *J. Hydraulic Engrg.*, ASCE, 118(1) (in press).

Camfield, F.E. (1977). "Wind-wave propagation over flooded, vegetated land." *Tech. Paper*

No. 77-12, Coast. Engrg. Res. Ctr., U.S. Army Engineer Waterways Experiment Station, Vicksburg, Miss.

Dalrymple, R.A., Kirby, J.T. and Hwang, P.A. (1984). "Wave diffraction due to areas of energy dissipation." *J. Wtrway. Port Coast. and Oc. Engrg.*, ASCE, 110(1), 67–79.

Dean, R.G. and Dalrymple, R.A. (1984). *Water Wave Mechanics for Engineers and Scientists.* World Scientific Publ. Co., Singapore.

Iwagaki, Y. and Tsuchiya, Y. (1966). "Laminar damping of oscillatory waves due to bottom friction." *Proc. 10th Coast. Engrg. Conf.*, ASCE, 1, 149–174.

Press, W.H., Flannery, B.P., Teukolsky, S.A. and Vetterling, W.T. (1986). *Numerical Recipes: The Art of Scientific Computing.* Cambridge Univ. Press, Cambridge, U.K.

Price, W.A., Tomlinson, K.W. and Hunt, J.N. (1968). "The effect of artificial seaweed in promoting the build-up of beaches." *Proc. 11th Coast. Engrg. Conf.*, ASCE, 1, 570–578.

Shore Protection Manual (1984). U.S. Army Coast. Engrg. Res. Ctr., 1, Government Printing Office, Washington, D.C.

APPENDIX A

COMPUTER PROGRAM FOR COMPUTING WAVE NUMBER AND EXPONENTIAL DECAY COEFFICIENT

This computer program computes the approximate value of k'_r for given L'_o using Eq. 31 for $\epsilon \ll 1$ and the approximate value of k'_i for given L'_o, d' and ϵ using Eq. 32 for $\epsilon \ll 1$ where ϵ is computed using Eq. 56 for given d', C_D and $\beta = bN\ H_o/2$ together with the computed approximate value of k'_r. This program also computes the exact values of k'_r and k'_i for given L'_o, d' and ϵ using Eq. 28 with Eqs. 27 and 29 where use is made of a Newton-Raphson iteration method starting from the approximate values of k'_r and k'_i.

The following input parameters need to be specified:

- beta = $\beta = b\ N\ H_o/2$ = dimensionless vegetation parameter
- ld = $L'_o = g/[2\pi(d+h)f^2]$ = dimensionless wave length
- dd = $d' = d/(d+h)$ = dimensionless depth
- cd = C_D = drag coefficient

The computer program writes the following output parameters:

- eps = ϵ = dimensionless damping coefficient given by Eq. 56
- krd = approximate value of $k'_r = k_r(d+h)$
- kid = approximate value of $k'_i = k_i(d+h)$
- kexact = exact value of $k'_r = k_r(d+h)$
- kexacti = exact value of $k'_i = k_i(d+h)$
- ratio1 = krd/kexact
- ratio2 = kid/kexacti

It should be noted that the computer program can easily be modified to compute the approximate and exact values of k'_r and k'_i for given L'_o, d' and ϵ instead of L'_o, d', β and C_D.

```
c     ****************************************************************
c           THIS PROGRAM COMPUTES AND OUTPUTS NORMALIZED WAVENUMBERS
c           FOR WAVES OVER VEGETATION, GIVEN DIMENSIONLESS INPUT
c
c           Output File - final.dat
c
c           INPUT
c
c           dd=dimensionless depth      ld=dimensionless wavelength
c           cd=drag coefficient         beta
c
c           OUTPUT
c
c           krd=approximate  real wavenumber
c           kid=approximate imaginary wavenumber
c           kexact=exact real wavenumber
c           kexacti=exact imaginary  wavenumber
c           ratio1=ratio of approximate to exact real wave #
c           ratio2=ratio of approximate to exact imaginary wave #
c
c     ****************************************************************
      implicit double precision (a-z)
      double precision kexacti,kexact,kid,krd
      open (unit=12,file='final.dat')
      write(6,*)'input beta'
      read(5,*)beta
      write(6,*)'input dimensionless wavelength'
      read(5,*)ld
      write(6,*)'input dimensionless depth (d/(h+d))'
      read(5,*)dd
      write(6,*)'input drag coefficient'
      read(5,*)cd
      pi=4d0*datan(1d0)

c          Output

      write (12,*) 'INPUT '
      write (12,*)
      write (12,81)cd,beta,dd,ld
      write (12,*)'  '
      write (12,*)'OUTPUT'
      write (12,*) ' '

c           computation of approximate and exact real and
c           imaginary wavenumbers

            c1=(2d0)*pi/ld
            call approx(dd,eps,krd,kid,c1,beta,
     1           cd,pi)
            call exact (dd,eps,krd,kid,c1,
     1           kexact,kexacti,ld)
            ratio1=krd/kexact
            ratio2=kid/kexacti
            write (12,*) "        kr'     "
            write (12,82) eps,krd,kexact,ratio1
            write (12,*) '   '
            write (12,*) "        ki'     "
            write (12,82) eps,kid,kexacti,ratio2

 20    continue

 81   format (1x,'CD=',f6.3,3x,'BETA=',f6.3,3x,"D'=",f6.3,3x,"Lo'=",f6.3,/)
 82   format (2x,'epsilon=',f5.3,3x,'approximate=',f6.3,
     1          4x,'exact=',f6.3,3x,'ratio=',f6.3)
      end
```

```
c       ++++++++++++++++++++++++++++++++++++++++++++++++++++++++++++++
c            SUBROUTINE TO COMPUTE REAL AND IMAGINARY PARTS OF
c            APPROXIMATE WAVE NUMBER
c       ++++++++++++++++++++++++++++++++++++++++++++++++++++++++++++++
c

        subroutine approx(d2d,eps,krd,kid,c1,beta,cd,pi)
        implicit double precision(a-z)

c

c            function statements for use in Newton Raphson computation

        f(x,y)=x*tanh(x)-y
        df(x)=tanh(x)+(x/(cosh(x)**2))
        err(x,y)=dabs(x-y)
        error=1**(-6)
c
c
c        calculation of initial guess(krd0) for Newton Raphson calculation

        if (c1.lt.1.0)then
           krd0=dsqrt(c1)
        else
           krd0=c1
        endif
c
c            Newton Raphson calculation for real part(krd) of wave number

 10     krd=krd0-(f(krd0,c1)/df(krd0))
       .if (err(krd,krd0).lt.error)then
        else
           krd0=krd
           goto 10
        endif
c
c            Calculation of imaginary part of wave number

        c2d=2.*krd*d2d
        b=krd*d2d
        a1=2./(9.*pi)*cd*beta
        eps=a1*(dsinh(3.*b)+(9.*dsinh(b)))/
     1  (((2.*b)+dsinh(2.*b))*(dsinh(krd)))
        kid=eps*krd*((c2d+dsinh(c2d))/((2*krd)+dsinh(2*krd)))

c
        return
        end

c       ++++++++++++++++++++++++++++++++++++++++++++++++++++++++++++++++
c
c            SUBROUTINE TO COMPUTE REAL AND IMAGINARY PARTS OF EXACT
c            WAVE NUMBER
c
c       ++++++++++++++++++++++++++++++++++++++++++++++++++++++++++++++++

        subroutine exact(d2d,eps,krd,kid,c1,kexact,kexacti,ld)
        implicit double precision (a-z)
        complex*16 t1,s1,ctanh,ccosh,z,z0,cf,cdf,ceps,a1,t2,s2,
     1      a2
c
c            function definitions for calculation simplification

        t1(c2,z0)=ctanh(c2*z0)
```

```
      t2(a2,z0)=ctanh(a2*z0)
      s1(c2,z0)=1d0/((ccosh(c2*z0))**2d0)
      s2(a2,z0)=1d0/((ccosh(a2*z0))**2d0)
c
c     function definitions for use in Newton-Raphson calculation

      cf(z0,a1,a2,c1,c2)=z0*(t1(c2,z0)+a1*t2(a2,z0))-c1*(1d0+a1*t2(a2,z0)
     1     *t1(c2,z0))
      cdf(z0,a1,a2,c1,c2)=t1(c2,z0)+a1*t2(a2,z0)+z0*((c2*s1(c2,z0))
     1     +(a1*a2*s2(a2,z0)))-c1*a1*((a2*t1(c2,z0)*s2(a2,z0))
     1     +(t2(a2,z0)*c2*s1(c2,z0)))
      realerr(z,z0)=dabs(dreal(z)-dreal(z0))
      imerr(z,z0)=dabs(dimag(z)-dimag(z0))
      error=1**(-6)
c
c          calculation of constants

      c2=1-d2d
      eps1=2.*eps
      ceps=dcmplx(1d0,eps1)
      a1=ceps**(-0.5)
      a2=a1*d2d
c
c          initial guess for Newton-Raphson calculation

      z0=dcmplx(krd,kid)
c
c          Newton -Raphson calculation

 200  z=z0-(cf(z0,a1,a2,c1,c2)/cdf(z0,a1,a2,c1,c2))
      if ((realerr(z,z0).lt.error).and.(imerr(z,z0).lt.error))then
      else
          z0=z
          goto 200
      endif
      kexact=dreal(z)
      kexacti=dimag(z)
      return
      end

c     ++++++++++++++++++++++++++++++++++++++++++++++++++++++++++++++++
c
c          DEFINITION OF COMPLEX HYPERBOLIC FUNCTIONS
c
c     ++++++++++++++++++++++++++++++++++++++++++++++++++++++++++++++++

      function ccosh(z0)
          complex*16 z0, ccosh
          double precision a,b
          a=dreal(z0)
          b=dimag(z0)
          ccosh=dcmplx(dcosh(a)*dcos(b),dsinh(a)*dsin(b))
          return
      end

      function ctanh(z0)
          complex*16 z0,ctanh
          double precision a,b,denom
          a=dreal(z0)
          b=dimag(z0)
          denom=(dcosh(2*a)+dcos(2*b))
          ctanh=dcmplx((dsinh(2*a))/denom,(dsin(2*b))/denom)
          return
      end
```

APPENDIX B

REGRESSION ANALYSIS OF MEASURED WAVE HEIGHTS FOR EACH OF SIXTY TEST RUNS

For each of sixty runs, the following quantities are listed:

- $k_i = KI$ = fitted exponential decay coefficient (cm^{-1})
- $H_o = HO$ = fitted wave height at $x = 0$ (cm)
- Measured wave heights H (cm) at $x = 0$, 200, 400 and 600 cm
- Fitted wave heights H (cm) at $x = 0$, 200, 400 and 600 cm using Eq. 17
- Correlation coefficient indicating the degree of the fit.

AVERAGE CORRELATION COEFFICIENT=0.959
BEST CORRELATION COEFFICIENT=0.998
WORST CORRELATION COEFFICIENT=0.780

RUN # 1

KI=.000439(cm-1) H0= 3.60(cm)

X(cm)	0.	200.	400.	600.
MEASURED H (cm)	3.800	3.100	2.900	2.900
FITTED H (cm)	3.599	3.296	3.019	2.766

CORRELATION COEFFICIENT=0.894

RUN # 2

KI=.000887(cm-1) H0=10.94(cm)

X(cm)	0.	200.	400.	600.
MEASURED H (cm)	10.800	9.500	7.400	6.500
FITTED H (cm)	10.935	9.158	7.670	6.424

CORRELATION COEFFICIENT=0.991

RUN # 3

KI=.000862(cm-1) H0= 7.31(cm)

X(cm)	0.	200.	400.	600.
MEASURED H (cm)	7.200	6.400	5.000	4.400
FITTED H (cm)	7.308	6.151	5.177	4.357

CORRELATION COEFFICIENT=0.989

RUN # 4

KI=.000902(cm-1) H0=13.38(cm)

X(cm)	0.	200.	400.	600.
MEASURED H (cm)	13.600	10.700	9.700	7.700
FITTED H (cm)	13.385	11.175	9.330	7.789

CORRELATION COEFFICIENT=0.988

RUN # 5

KI=.000756(cm-1) H0= 8.44(cm)

X(cm)	0.	200.	400.	600.
MEASURED H (cm)	8.400	7.100	6.600	5.200
FITTED H (cm)	8.438	7.254	6.237	5.362

CORRELATION COEFFICIENT=0.983

RUN # 6

KI=.000901(cm-1) H0=14.34(cm)

X(cm)	0.	200.	400.	600.
MEASURED H (cm)	14.700	11.600	9.900	8.500
FITTED H (cm)	14.341	11.977	10.002	8.353

CORRELATION COEFFICIENT=0.993

RUN # 7

KI=.000704(cm-1) H0= 8.69(cm)

X(cm)	0.	200.	400.	600.
MEASURED H (cm)	8.900	7.200	6.700	5.700
FITTED H (cm)	8.688	7.547	6.555	5.694

CORRELATION COEFFICIENT=0.983

RUN # 8

KI=.000919(cm-1) H0=18.85(cm)

X(cm)	0.	200.	400.	600.
MEASURED H (cm)	19.300	15.300	12.800	11.100
FITTED H (cm)	18.855	15.689	13.055	10.863

CORRELATION COEFFICIENT=0.994

RUN # 9

KI=.001011(cm-1) H0=17.59(cm)

X(cm)	0.	200.	400.	600.
MEASURED H (cm)	18.400	13.700	11.300	10.000
FITTED H (cm)	17.594	14.373	11.742	9.593

CORRELATION COEFFICIENT=0.983

RUN # 10

KI=.000824(cm-1) H0=13.75(cm)

X(cm)	0.	200.	400.	600.
MEASURED H (cm)	14.000	11.400	9.800	8.500
FITTED H (cm)	13.750	11.660	9.888	8.386

CORRELATION COEFFICIENT=0.996

RUN # 11

KI=.000677(cm-1) H0=11.77(cm)

X(cm)	0.	200.	400.	600.
MEASURED H (cm)	12.200	10.000	8.500	8.200
FITTED H (cm)	11.766	10.276	8.974	7.837

CORRELATION COEFFICIENT=0.970

RUN # 12

KI=.000774(cm-1) H0=10.47(cm)

X(cm)	0.	200.	400.	600.
MEASURED H (cm)	10.600	8.900	7.500	6.700
FITTED H (cm)	10.466	8.965	7.680	6.579

CORRELATION COEFFICIENT=0.996

RUN # 13

KI=.000770(cm-1) H0= 8.65(cm)

X(cm)	0.	200.	400.	600.
MEASURED H (cm)	8.900	7.200	6.200	5.600
FITTED H (cm)	8.652	7.417	6.359	5.452

CORRELATION COEFFICIENT=0.988

RUN # 14

KI=.000734(cm-1) H0= 7.22(cm)

X(cm)	0.	200.	400.	600.
MEASURED H (cm)	7.400	6.000	5.400	4.700
FITTED H (cm)	7.220	6.235	5.384	4.649

CORRELATION COEFFICIENT=0.989

RUN # 15

KI=.000560(cm-1) H0= 4.84(cm)

X(cm)	0.	200.	400.	600.
MEASURED H (cm)	5.000	4.100	3.900	3.500
FITTED H (cm)	4.838	4.326	3.867	3.457

CORRELATION COEFFICIENT=0.967

RUN # 16

KI=.000733(cm-1) H0=13.67(cm)

X(cm)	0.	200.	400.	600.
MEASURED H (cm)	14.000	11.500	10.000	9.000
FITTED H (cm)	13.668	11.806	10.196	8.807

CORRELATION COEFFICIENT=0.990

RUN # 17

KI=.000578(cm-1) H0= 8.14(cm)

X(cm)	0.	200.	400.	600.
MEASURED H (cm)	8.200	7.200	6.400	5.800
FITTED H (cm)	8.138	7.249	6.458	5.752

CORRELATION COEFFICIENT=0.998

RUN # 18

KI=.000465(cm-1) H0=13.89(cm)

X(cm)	0.	200.	400.	600.
MEASURED H (cm)	13.800	12.700	11.700	10.400
FITTED H (cm)	13.895	12.660	11.535	10.510

CORRELATION COEFFICIENT=0.996

RUN # 19

KI=.000388(cm-1) H0= 8.84(cm)

X(cm)	0.	200.	400.	600.
MEASURED H (cm)	9.000	8.000	7.500	7.100
FITTED H (cm)	8.840	8.180	7.569	7.004

CORRELATION COEFFICIENT=0.982

RUN # 20

KI=.000298(cm-1) H0= 9.46(cm)

X(cm)	0.	200.	400.	600.
MEASURED H (cm)	9.800	8.400	8.500	8.000
FITTED H (cm)	9.460	8.912	8.395	7.909

CORRELATION COEFFICIENT=0.885

RUN # 21

KI=.000373(cm-1) H0= 6.52(cm)

X(cm)	0.	200.	400.	600.
MEASURED H (cm)	6.600	6.000	5.500	5.300
FITTED H (cm)	6.518	6.050	5.616	5.212

CORRELATION COEFFICIENT=0.985

RUN # 22

KI=.000356(cm-1) H0= 7.93(cm)

X(cm)	0.	200.	400.	600.
MEASURED H (cm)	8.200	7.000	6.900	6.500
FITTED H (cm)	7.925	7.381	6.874	6.402

CORRELATION COEFFICIENT=0.926

RUN # 23

KI=.000540(cm-1) H0= 8.75(cm)

X(cm)	0.	200.	400.	600.
MEASURED H (cm)	8.600	8.100	7.000	6.300
FITTED H (cm)	8.754	7.858	7.054	6.332

CORRELATION COEFFICIENT=0.987

RUN # 24

KI=.000420(cm-1) H0= 5.56(cm)

X(cm)	0.	200.	400.	600.
MEASURED H (cm)	5.500	5.200	4.700	4.300
FITTED H (cm)	5.561	5.113	4.702	4.323

CORRELATION COEFFICIENT=0.993

RUN # 25

KI=.000473(cm-1) H0=11.04(cm)

X(cm)	0.	200.	400.	600.
MEASURED H (cm)	11.500	9.800	8.500	8.800
FITTED H (cm)	11.041	10.046	9.140	8.316

CORRELATION COEFFICIENT=0.914

RUN # 26

KI=.000390(cm-1) H0= 6.76(cm)

X(cm)	0.	200.	400.	600.
MEASURED H (cm)	6.900	6.400	5.200	5.700
FITTED H (cm)	6.762	6.254	5.785	5.350

CORRELATION COEFFICIENT=0.838

RUN # 27

KI=.000523(cm-1) H0=14.41(cm)

X(cm)	0.	200.	400.	600.
MEASURED H (cm)	14.400	13.200	11.300	10.700
FITTED H (cm)	14.405	12.974	11.685	10.524

CORRELATION COEFFICIENT=0.987

RUN # 28

KI=.000484(cm-1) H0= 9.19(cm)

X(cm)	0.	200.	400.	600.
MEASURED H (cm)	9.300	8.300	7.400	7.000
FITTED H (cm)	9.193	8.346	7.577	6.878

CORRELATION COEFFICIENT=0.991

RUN # 29

KI=.000602(cm-1) H0=19.38(cm)

X(cm)	0.	200.	400.	600.
MEASURED H (cm)	19.000	17.600	15.400	13.300
FITTED H (cm)	19.378	17.181	15.233	13.505

CORRELATION COEFFICIENT=0.990

RUN # 30

KI=.000536(cm-1) H0=16.82(cm)

X(cm)	0.	200.	400.	600.
MEASURED H (cm)	16.600	15.400	13.600	12.100
FITTED H (cm)	16.822	15.111	13.573	12.193

CORRELATION COEFFICIENT=0.994

RUN # 31

KI=.000454(cm-1) H0=14.22(cm)

X(cm)	0.	200.	400.	600.
MEASURED H (cm)	13.900	13.300	12.100	10.600
FITTED H (cm)	14.219	12.985	11.859	10.830

CORRELATION COEFFICIENT=0.976

RUN # 32

KI=.000454(cm-1) H0=12.31(cm)

X(cm)	0.	200.	400.	600.
MEASURED H (cm)	11.900	11.800	10.300	9.200
FITTED H (cm)	12.307	11.239	10.264	9.373

CORRELATION COEFFICIENT=0.948

RUN # 33

KI=.000396(cm-1) H0= 9.70(cm)

X(cm)	0.	200.	400.	600.
MEASURED H (cm)	9.600	9.100	8.300	7.600
FITTED H (cm)	9.704	8.964	8.281	7.650

CORRELATION COEFFICIENT=0.993

RUN # 34

KI=.000354(cm-1) H0= 6.98(cm)

X(cm)	0.	200.	400.	600.
MEASURED H (cm)	6.800	6.800	6.000	5.600
FITTED H (cm)	6.981	6.504	6.060	5.646

CORRELATION COEFFICIENT=0.940

RUN # 35

KI=.000436(cm-1) H0=17.16(cm)

X(cm)	0.	200.	400.	600.
MEASURED H (cm)	17.100	15.700	14.600	13.100
FITTED H (cm)	17.157	15.724	14.411	13.208

CORRELATION COEFFICIENT=0.997

RUN # 36

KI=.000438(cm-1) H0=11.58(cm)

X(cm)	0.	200.	400.	600.
MEASURED H (cm)	11.700	10.500	9.600	9.000
FITTED H (cm)	11.577	10.605	9.715	8.899

CORRELATION COEFFICIENT=0.994

RUN # 37

KI=.000343(cm-1) H0=17.04(cm)

X(cm)	0.	200.	400.	600.
MEASURED H (cm)	16.900	16.100	14.900	13.800
FITTED H (cm)	17.045	15.916	14.861	13.877

CORRELATION COEFFICIENT=0.994

RUN # 38

KI=.000294(cm-1) H0= 9.58(cm)

X(cm)	0.	200.	400.	600.
MEASURED H (cm)	9.200	9.400	8.900	7.700
FITTED H (cm)	9.584	9.036	8.520	8.033

CORRELATION COEFFICIENT=0.833

RUN # 39

KI=.000314(cm-1) H0=12.19(cm)

X(cm)	0.	200.	400.	600.
MEASURED H (cm)	11.900	11.900	10.700	10.000
FITTED H (cm)	12.191	11.449	10.752	10.097

CORRELATION COEFFICIENT=0.942

RUN # 40

KI=.000168(cm-1) H0= 7.56(cm)

X(cm)	0.	200.	400.	600.
MEASURED H (cm)	7.400	7.600	7.000	6.800
FITTED H (cm)	7.565	7.315	7.073	6.840

CORRELATION COEFFICIENT=0.844

RUN # 41

KI=.000194(cm-1) H0= 8.07(cm)

X(cm)	0.	200.	400.	600.
MEASURED H (cm)	7.800	8.100	7.600	7.000
FITTED H (cm)	8.071	7.763	7.468	7.183

CORRELATION COEFFICIENT=0.796

RUN # 42

KI=.000364(cm-1) H0= 6.28(cm)

X(cm)	0.	200.	400.	600.
MEASURED H (cm)	6.500	5.500	5.500	5.100
FITTED H (cm)	6.276	5.836	5.426	5.045

CORRELATION COEFFICIENT=0.917

RUN # 43

KI=.000252(cm-1) H0= 3.90(cm)

X(cm)	0.	200.	400.	600.
MEASURED H (cm)	4.100	3.500	3.400	3.500
FITTED H (cm)	3.899	3.707	3.525	3.352

CORRELATION COEFFICIENT=0.780

RUN # 44

KI=.000754(cm-1) H0=10.01(cm)

X(cm)	0.	200.	400.	600.
MEASURED H (cm)	10.000	8.800	7.100	6.500
FITTED H (cm)	10.008	8.608	7.404	6.368

CORRELATION COEFFICIENT=0.990

RUN # 45

KI=.000544(cm-1) H0= 6.02(cm)

X(cm)	0.	200.	400.	600.
MEASURED H (cm)	6.000	5.500	4.700	4.400
FITTED H (cm)	6.017	5.397	4.841	4.342

CORRELATION COEFFICIENT=0.989

RUN # 46

KI=.000597(cm-1) H0=12.03(cm)

X(cm)	0.	200.	400.	600.
MEASURED H (cm)	12.300	10.200	9.700	8.400
FITTED H (cm)	12.028	10.674	9.472	8.406

CORRELATION COEFFICIENT=0.978

RUN # 47

KI=.000400(cm-1) H0= 7.04(cm)

X(cm)	0.	200.	400.	600.
MEASURED H (cm)	7.300	6.000	6.300	5.500
FITTED H (cm)	7.038	6.496	5.997	5.535

CORRELATION COEFFICIENT=0.874

RUN # 48

KI=.000536(cm-1) H0=16.15(cm)

X(cm)	0.	200.	400.	600.
MEASURED H (cm)	16.500	14.000	13.100	11.800
FITTED H (cm)	16.145	14.504	13.029	11.704

CORRELATION COEFFICIENT=0.983

RUN # 49

KI=.000516(cm-1) H0=14.20(cm)

X(cm)	0.	200.	400.	600.
MEASURED H (cm)	14.500	12.500	11.400	10.600
FITTED H (cm)	14.202	12.809	11.553	10.421

CORRELATION COEFFICIENT=0.986

RUN # 50

KI=.000428(cm-1) H0=12.50(cm)

X(cm)	0.	200.	400.	600.
MEASURED H (cm)	12.800	11.100	10.500	9.800
FITTED H (cm)	12.504	11.477	10.535	9.670

CORRELATION COEFFICIENT=0.975

RUN # 51

KI=.000542(cm-1) H0=11.15(cm)

X(cm)	0.	200.	400.	600.
MEASURED H (cm)	11.300	9.800	9.000	8.100
FITTED H (cm)	11.153	10.007	8.979	8.056

CORRELATION COEFFICIENT=0.994

RUN # 52

KI=.000432(cm-1) H0= 8.78(cm)

X(cm)	0.	200.	400.	600.
MEASURED H (cm)	9.000	7.800	7.300	6.900
FITTED H (cm)	8.777	8.051	7.385	6.775

CORRELATION COEFFICIENT=0.973

RUN # 53

KI=.000368(cm-1) H0= 6.90(cm)

X(cm)	0.	200.	400.	600.
MEASURED H (cm)	7.000	6.300	5.900	5.600
FITTED H (cm)	6.898	6.410	5.955	5.533

CORRELATION COEFFICIENT=0.986

RUN # 54

KI=.000450(cm-1) H0=14.46(cm)

X(cm)	0.	200.	400.	600.
MEASURED H (cm)	14.500	13.100	12.200	11.000
FITTED H (cm)	14.462	13.217	12.080	11.040

CORRELATION COEFFICIENT=0.998

RUN # 55

KI=.000412(cm-1) H0= 9.10(cm)

X(cm)	0.	200.	400.	600.
MEASURED H (cm)	9.200	8.300	7.600	7.200
FITTED H (cm)	9.097	8.378	7.716	7.106

CORRELATION COEFFICIENT=0.992

RUN # 56

KI=.000263(cm-1) H0=15.07(cm)

X(cm)	0.	200.	400.	600.
MEASURED H (cm)	15.300	14.000	13.500	13.000
FITTED H (cm)	15.065	14.295	13.564	12.870

CORRELATION COEFFICIENT=0.972

RUN # 57

KI=.000221(cm-1) H0= 8.70(cm)

X(cm)	0.	200.	400.	600.
MEASURED H (cm)	8.700	8.300	8.000	7.600
FITTED H (cm)	8.698	8.322	7.962	7.617

CORRELATION COEFFICIENT=0.998

RUN # 58

KI=.000255(cm-1) H0=11.39(cm)

X(cm)	0.	200.	400.	600.
MEASURED H (cm)	11.700	10.500	10.100	10.000
FITTED H (cm)	11.393	10.827	10.289	9.777

CORRELATION COEFFICIENT=0.919

RUN # 59

KI=.000147(cm-1) H0= 6.08(cm)

X(cm)	0.	200.	400.	600.
MEASURED H (cm)	6.100	5.800	5.900	5.500
FITTED H (cm)	6.083	5.907	5.736	5.570

CORRELATION COEFFICIENT=0.876

RUN # 60

KI=.000218(cm-1) H0= 6.82(cm)

X(cm)	0.	200.	400.	600.
MEASURED H (cm)	6.900	6.400	6.300	6.000
FITTED H (cm)	6.823	6.532	6.254	5.988

CORRELATION COEFFICIENT=0.969
